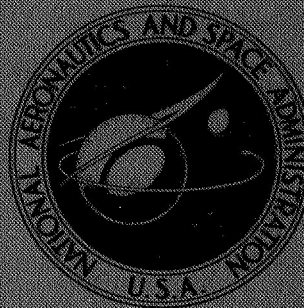


NASA CONTRACTOR  
REPORT



NASA CR-763

NASA CR-763

FACILITY FORM 602

N67-23718  
(ACCESSION NUMBER)

46  
(PAGES)

CR-763  
(NASA CR OR TMX OR AD NUMBER)

(THRU)

(CODE)

10  
(CATEGORY)

STUDY OF DIODE-IRIS CONTROLLED  
WAVEGUIDE SLOT RADIATORS

by B. J. Forman, J. Y. Wada, and W. H. Kummer

Prepared by  
HUGHES AIRCRAFT COMPANY  
Culver City, Calif.  
for Langley Research Center

3 STUDY OF DIODE-IRIS CONTROLLED WAVEGUIDE SLOT RADIATORS 6

By B. J. Forman, J. Y. Wada, and W. H. Kummer 8

Distribution of this report is provided in the interest of information exchange. Responsibility for the contents resides in the author or organization that prepared it.

25  
27  
Prepared under Contract No. NAS 1-4053 by  
1 HUGHES AIRCRAFT COMPANY  
Culver City, Calif. 3

for Langley Research Center

NATIONAL AERONAUTICS AND SPACE ADMINISTRATION

---

For sale by the Clearinghouse for Federal Scientific and Technical Information  
Springfield, Virginia 22151 - CFSTI price \$3.00

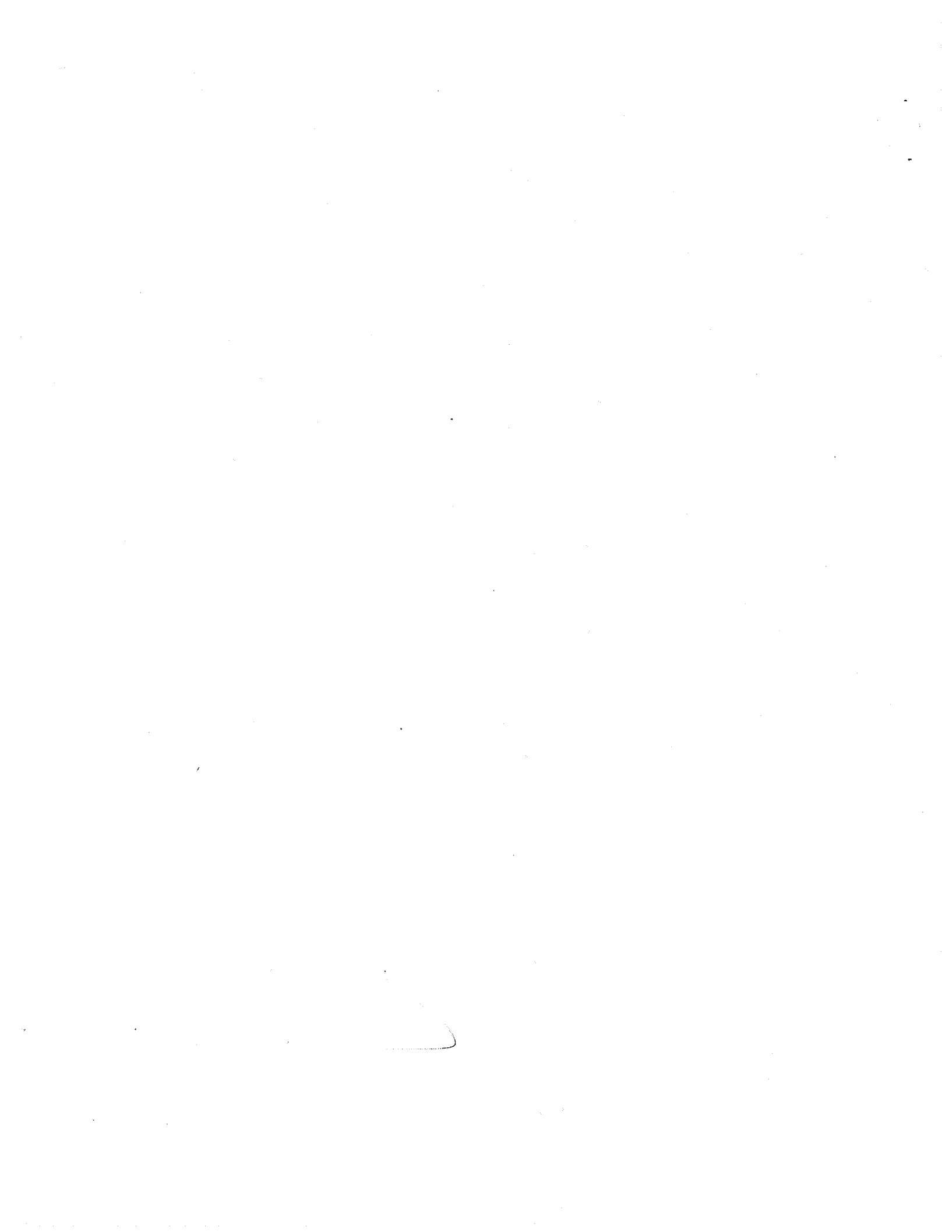


## SUMMARY

X-band studies concerned with positioning semiconductor diodes and plasma devices about a slot radiator to control the amplitude and phase of the slot radiation were continued in this program from Contract No. NAS 1-2621, April 1964.

An iris cluster of four semiconductor varactor diodes was developed that produced 360 degrees of phase control at amplitude levels up to -14.5 db (relative to the incident power) and less phase control for amplitudes up to -7.8 db. The VSWR response never exceeded 1.55:1, and the nominal ohmic loss varied from 14.5 to 8.1 percent. Six-volt varactors operated satisfactorily at r-f power levels to 0.1 milliwatt while lossier, 40-volt versions functioned at 1.0 milliwatt. A five-element, traveling-wave, linear array containing 6-volt diode irises was designed, fabricated, and tested. Diode-iris control provided  $\pm 60$  degrees of electronic beam scanning about broadside.

Feasibility studies with various gas discharge waveguide irises predicted an electron injection plasma varactor design capable of operation at substantial r-f power levels with a few watts drive power and very low ohmic loss. A four-plasma iris prototype displayed a 125-watt power handling capability and an average ohmic loss of 5 percent. This unit provided 360 degrees of slot phase control at coupling levels of -13 db and exhibited a VSWR variation below 1.73:1.



## CONTENTS

	Page
1.0 INTRODUCTION . . . . .	1
2.0 TECHNICAL DISCUSSION . . . . .	5
2.1 Semiconductor Diode-Iris Development . . . . .	5
2.1.1 Two-Diode Iris Configurations . . . . .	5
2.1.2 Four-Diode Iris Configurations . . . . .	10
2.1.3 Five-Element Array . . . . .	16
2.2 Plasma Iris Feasibility Investigation . . . . .	21
2.2.1 Theory of Plasma Varactors in Waveguides . . . . .	23
2.2.2 Cold Cathode Microdiode Design . . . . .	26
2.2.3 Positive Column Plasma Reactance Tube . . . . .	27
2.2.4 Electron Injection Plasma Varactors . . . . .	36
3.0 CONCLUSIONS . . . . .	39
4.0 REFERENCES . . . . .	41

## ILLUSTRATIONS

		Page
Figure 1.	Positions for electronically variable irises . . . . .	2
Figure 2.	Ferrite iris design . . . . .	3
Figure 3.	Semiconductor 4-diode iris design . . . . .	4
Figure 4.	Amplitude and loss measuring setup for 2-diode iris configurations . . . . .	6
Figure 5.	Coupling, loss, and VSWR response versus $h$ parameter for a 2-diode iris unit . . . . .	9
Figure 6.	Construction of post used to fasten diode near slot . . . . .	11
Figure 7.	Effect of r-f power level on slot coupling for 6-volt diodes . . . . .	11
Figure 8.	Effect of r-f power level on iris ohmic loss for 6-volt diodes . . . . .	12
Figure 9.	Effect of r-f power level on slot coupling for 40-volt diodes . . . . .	12
Figure 10.	Effect of r-f power level on iris ohmic loss for 40-volt diodes . . . . .	13
Figure 11.	Phase bridge circuit block diagram . . . . .	14
Figure 12.	Phase and amplitude variation of a 4-diode iris controlled slot radiator. . . . .	17
Figure 13.	Loss resonance effect in 4-diode iris design . . . . .	18
Figure 14.	A 4-diode iris controlled slot radiator . . . . .	19
Figure 15.	Five-element diode-iris array . . . . .	20
Figure 16.	Radiation patterns of 5-element array illustrating 120 degrees of electronic beam scanning by 4-diode iris control. . . . .	22
Figure 17.	Plasma microdiode design . . . . .	26
Figure 18.	R-f admittance characteristics of semiconductor and plasma varactors . . . . .	28
Figure 19.	Positive column plasma reactance tubes . . . . .	29
Figure 20.	Measured electrical characteristics of positive column plasma reactance tubes . . . . .	30
Figure 21.	Quality factor $Q$ versus discharge power for positive column plasma reactance tubes . . . . .	31
Figure 22.	Discharge power versus phase shift for positive column plasma reactance tubes . . . . .	32

	Page
Figure 23. Variable amplitude control units using 3-millimeter Bendix tubes as irises . . . . .	34
Figure 24. Coupling and loss data for variable amplitude control units using 3-millimeter Bendix tubes as irises . . . . .	35



# STUDY OF DIODE-IRIS CONTROLLED WAVEGUIDE SLOT RADIATORS

## 1.0 INTRODUCTION

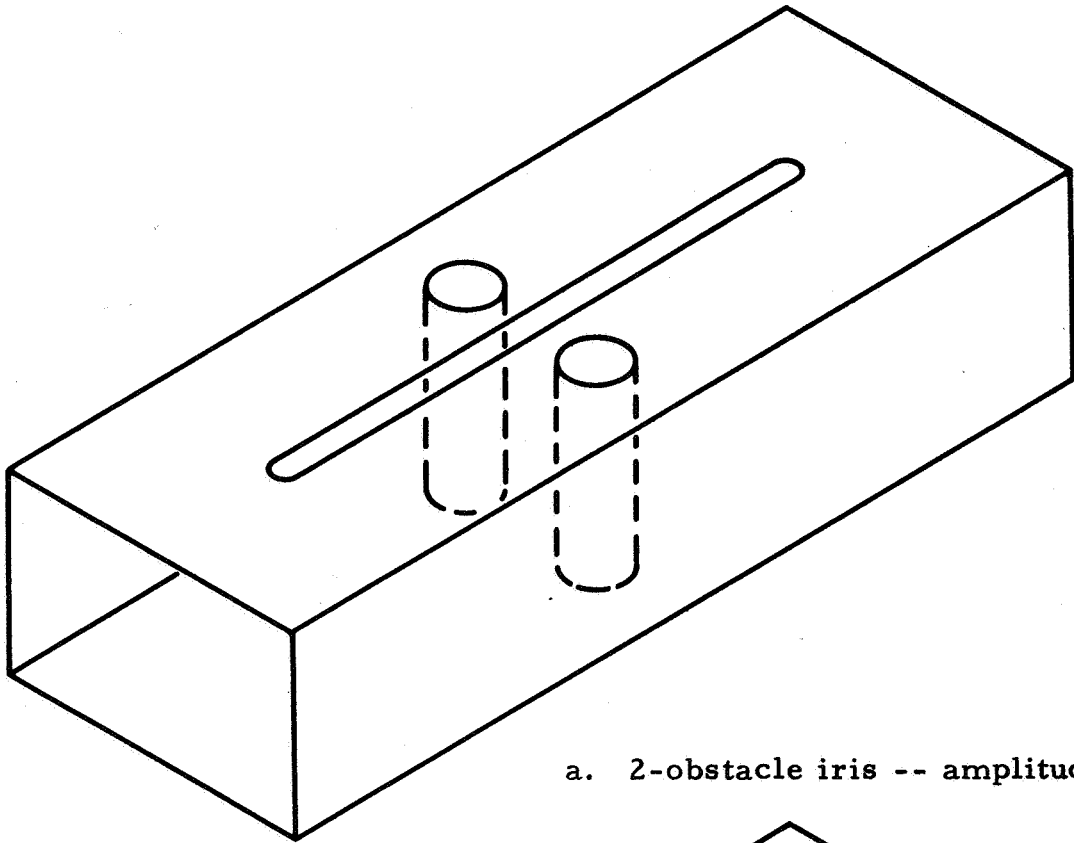
One method of electronically controlling the radiation from a waveguide slot radiator involves the use of an electronically operated waveguide iris. The iris must be located near the slot and be mounted in such a way that it perturbs the dominant rectangular waveguide mode into coupling through the slot. Two electronically variable obstacles located in the transverse waveguide plane which bisects the slot length (see Figure 1a) will provide amplitude control, but two pairs of such obstacles, disposed an equal distance in either direction from the midpoint of the slot length (see Figure 1b), will produce both amplitude and phase control.

In the past, magnetic-field controlled ferrites<sup>1</sup> (see Figure 2) and voltage-controlled semiconductor diodes<sup>2</sup> (see Figure 3) have been employed by researchers as irises for complete slot radiation control. Under NASA/Langley sponsorship\*, a ten-element, diode-controlled, linear array was built at the Hughes Aircraft Company that provided  $\pm 45$  degrees of beam scanning at X-band and monopulse patterns with an average iris ohmic (or dissipative) loss of 0.68 db. The present program is a combination of these studies with the objective of improving electronic-iris slot control in two ways: by pursuing further development of the semiconductor diode iris and by investigating the utility of using plasma discharge devices, such as cold cathode microdiodes and positive column plasma reactance tubes, as slot control irises. Included in this report is information on the degree of slot control, the ohmic and reflective loss, the r-f power handling capability, and the drive power requirements for both types of irises.

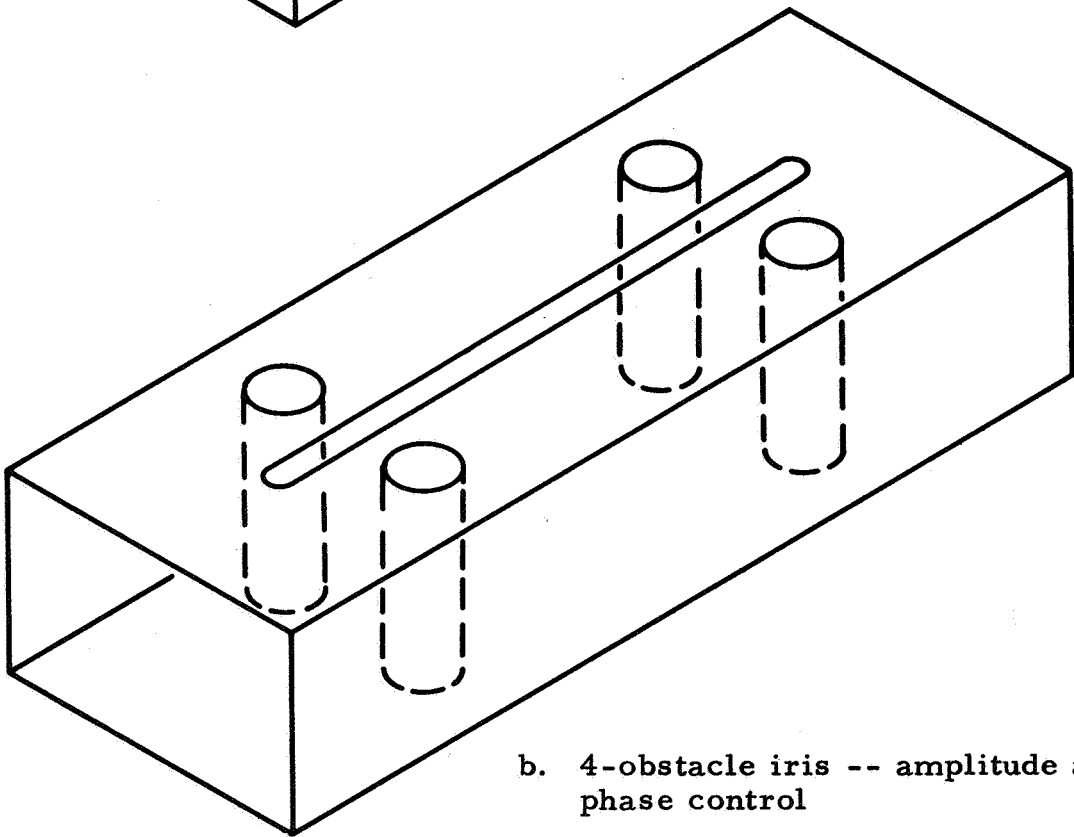
A brief summary is also presented of a study of electron injection plasma varactors, another possible type of plasma discharge control device. This study was performed concurrently with the NASA/Langley

---

\*Study of Advanced Antenna Techniques for Rendezvous Radar,  
NASA CR-764, 1967.



a. 2-obstacle iris -- amplitude control



b. 4-obstacle iris -- amplitude and phase control

Figure 1. Positions for electronically variable irises.

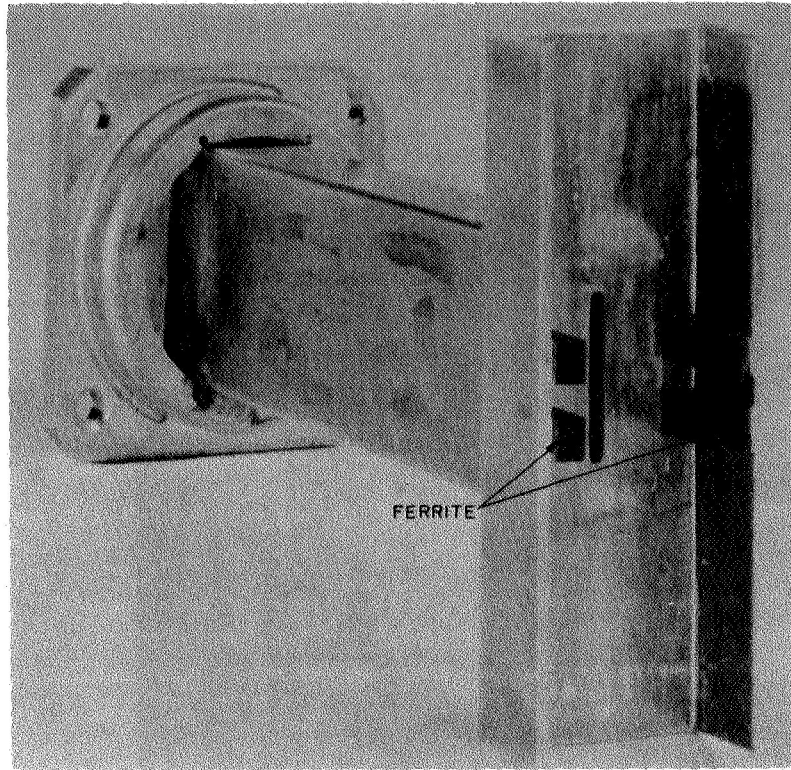


Figure 2. Ferrite iris design.

investigation as an internal research project funded by the Hughes Aircraft Company; results are presented to make this description of electronically controlled waveguide irises as complete and current as possible. Detailed discussions of the electron injection plasma varactors can be found in Research Report No. 322<sup>3</sup> and Special Research Report No. SRS-658<sup>4</sup>, both published by the Hughes Aircraft Company.

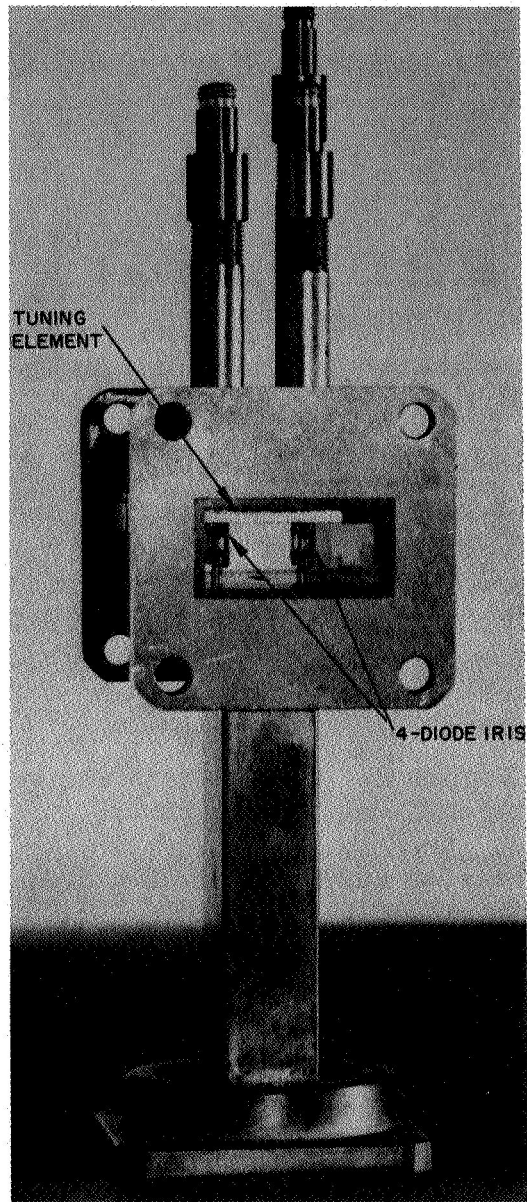


Figure 3. Semiconductor 4-diode iris design.

## 2.0 TECHNICAL DISCUSSION

The waveguide slot coupling study work was divided into two investigations: a semiconductor diode iris development investigation and a plasma iris feasibility investigation. Each is discussed separately below.

### 2.1 SEMICONDUCTOR DIODE-IRIS DEVELOPMENT

Development work with semiconductor diode irises at X-band was primarily experimental in nature and was concentrated on maximizing the iris control of slot radiation and minimizing the reflective and ohmic loss of the iris. To satisfy both factors within the limitations of current diode technology, an extensive systematic program was undertaken to vary the location and mounting of the diodes in the vicinity of the slot to reduce diode lead wire losses. Experiments with vertically mounted wires across a waveguide had indicated that losses from the diode lead wires could be substantial. Experimentation began with the collection and evaluation of design information on new two-diode iris configurations; these data were then applied to the design of individual four-diode iris devices. The best device was incorporated into the design of a five-element linear array.

#### 2.1.1 Two-Diode Iris Configurations

Coupling and loss measurements were performed on two-diode iris configurations in which the diode junctions were located in the transverse plane of the waveguide that bisects the slot length.

The measurement set-up used for taking the data is shown in Figure 4. The test device contained three waveguide ports with one located over the radiating slot to facilitate the measurement of slot radiation. Measurements of the net power transmitted and reflected from each port were obtained with this bench set-up and used to calculate such significant parameters as the fraction of incident power radiated from the slot and the corresponding fraction dissipated by the diode iris.

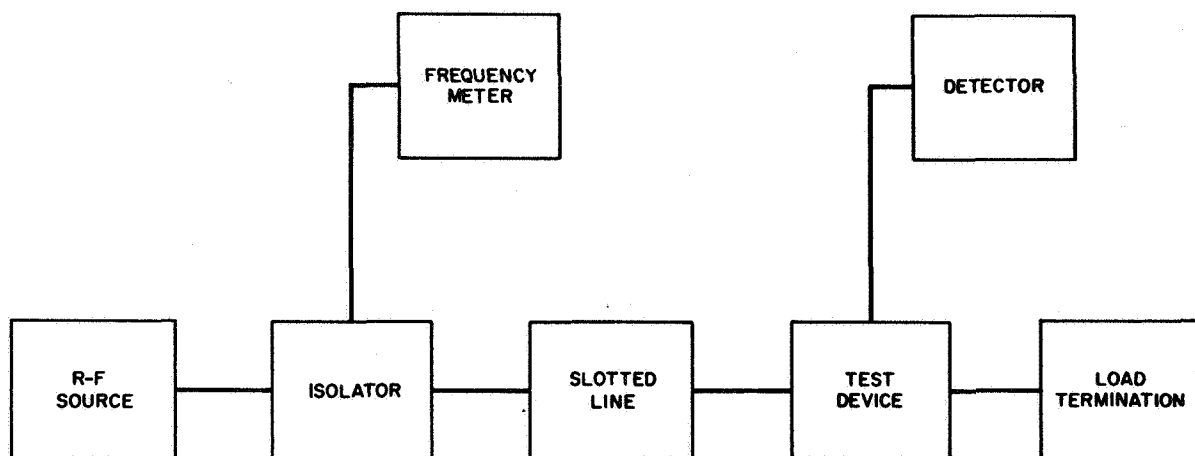


Figure 4. Amplitude and loss measuring setup for 2-diode iris configurations.

Various two-diode iris configurations were investigated to determine empirically the most appropriate geometrical arrangement for low loss and substantial coupling control. These included mounting the diodes horizontally and transversely on the broadwall containing the slot, horizontally and longitudinally between the broadwall containing the slot and the narrow wall of the waveguide, and horizontally and transversely on the broadwall opposite the slot. A schematic drawing and electrical data for each configuration measured are given in Table I. It can be seen that configuration No. 1 consistently provided sizable slot coupling values and exhibited low ohmic loss and low reflections.

The measured results on configuration No. 1 suggested that further development work focus on improving this configuration. Empirical investigations were made of several geometric parameters: the vertical distance  $h$  between the diodes and the broadwall containing the slot, the separation  $d$  between the diodes, the proximity of the diode junction to the slot for a given diode separation, the orientation

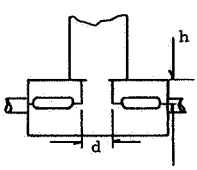
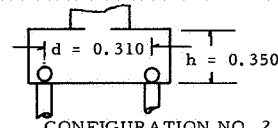
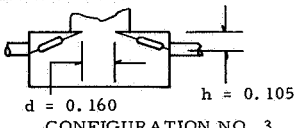
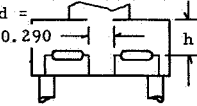
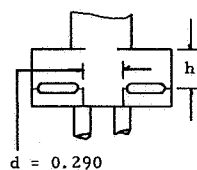
2-DIODE IRIS CONFIGURATIONS (Dimensions in Inches)	MAXIMUM SLOT COUPLING RELATIVE TO INPUT (db)	VSWR RESPONSE	OHMIC LOSS VARIATION (Percent Incident Power)	REMARKS	
 <p><math>d = 0.290</math></p> <p>CONFIGURATION NO. 1</p>	h (Inches)				
	0.105	-12.1	1.67:1 - 2.56:1	4.4 - 8.1	Minimum slot radiation with diodes forward biased
	0.105	-10.8	1.30:1 - 1.76:1	3.5 - 8.7	
	0.105	- 9.0	1.13:1 - 1.57:1	1.7 - 4.6	
	0.105	- 7.6	1.16:1 - 1.72:1	4.3 - 7.4	
	0.105	- 7.2	1.24:1 - 1.80:1	5.5 - 8.0	
	0.060	-12.4	1.06:1 - 1.31:1	3.3 - 7.2	
 <p><math>d = 0.310</math>    <math>h = 0.350</math></p> <p>CONFIGURATION NO. 2</p>	-31.2	<1.13:1	4.0 - 4.4		
 <p><math>d = 0.160</math>    <math>h = 0.105</math></p> <p>CONFIGURATION NO. 3</p>	-20.4	<1.15:1	1.7 - 3.1		
 <p><math>d = 0.290</math></p> <p>CONFIGURATION NO. 4</p>	h (Inches)				
	0.295	-13.2	12.3:1 - 16.2:1	6.0 - 9.8	
	0.350	-32.6	1.47:1 - 1.53:1	4.4 - 5.2	
 <p><math>d = 0.290</math></p> <p>CONFIGURATION NO. 5</p>	h (Inches)				
	0.050	None	> 20		
	0.200	-16.7	5.21:1 - 18.3:1		Minimum slot radiation with diodes forward biased
	0.200	-17.4	3.8:1 - 5.2:1	13.5 - 18.5	
	0.350	-24.6	1.29:1 - 1.47:1	1.3 - 2.4	Minimum slot radiation with diodes forward biased
	0.350	-24.6	1.14:1 - 1.31:1	2.1 - 3.0	

Table I. Data on 2-diode iris configurations.

of the diode whisker relative to the transverse plane of the waveguide, and the displacement of the shunt slot from the waveguide centerline.

It was determined that the  $d$  parameter and diode junction location exerted small influence on slot coupling. The parallel rather than perpendicular orientation of the plane of the diode whisker relative to the local transverse plane of the waveguide reduced the average ohmic loss by two percent; subsequent units contained diodes which were thus oriented for minimal loss. Shunt slot displacements were found to increase the coupling level on the slot displacement side of the waveguide but to substantially reduce it on the opposite side. Since this approach would produce unsymmetrical coupling and phase control, it was discarded.

The  $h$  parameter proved to be the most significant geometrical factor for slot coupling control. It primarily determined the level of slot coupling, the degree of mismatch, and the extent of ohmic loss. The influence of this parameter can be seen in Figure 5 in which an empirical compilation of the maximum slot coupling, VSWR response, and extreme variation in ohmic loss are graphically recorded. It is interesting to note that diode iris control increased with increased diode separation from the slot. The method of generating slot coupling by biasing the diodes from reverse to forward voltages rather than vice versa significantly reduced reflections and slightly lowered the ohmic loss of the configuration; this biasing procedure was adopted for all subsequent configurations.

The repeatability of the data was checked in two ways. First, the diodes were removed, reinserted, and the iris unit remeasured. Secondly, different diodes were used and the measurement procedure repeated. In the first check maximum slot coupling values repeated within 0.3 db with no overall change in VSWR and ohmic loss; in the second the VSWR and ohmic behavior remained invariant but the maximum slot coupling was reduced by 0.7 db. Both checks were repeated several times with the same degree of success. This information illustrates the degree of repeatability obtained by using diode iris slot coupling control devices.



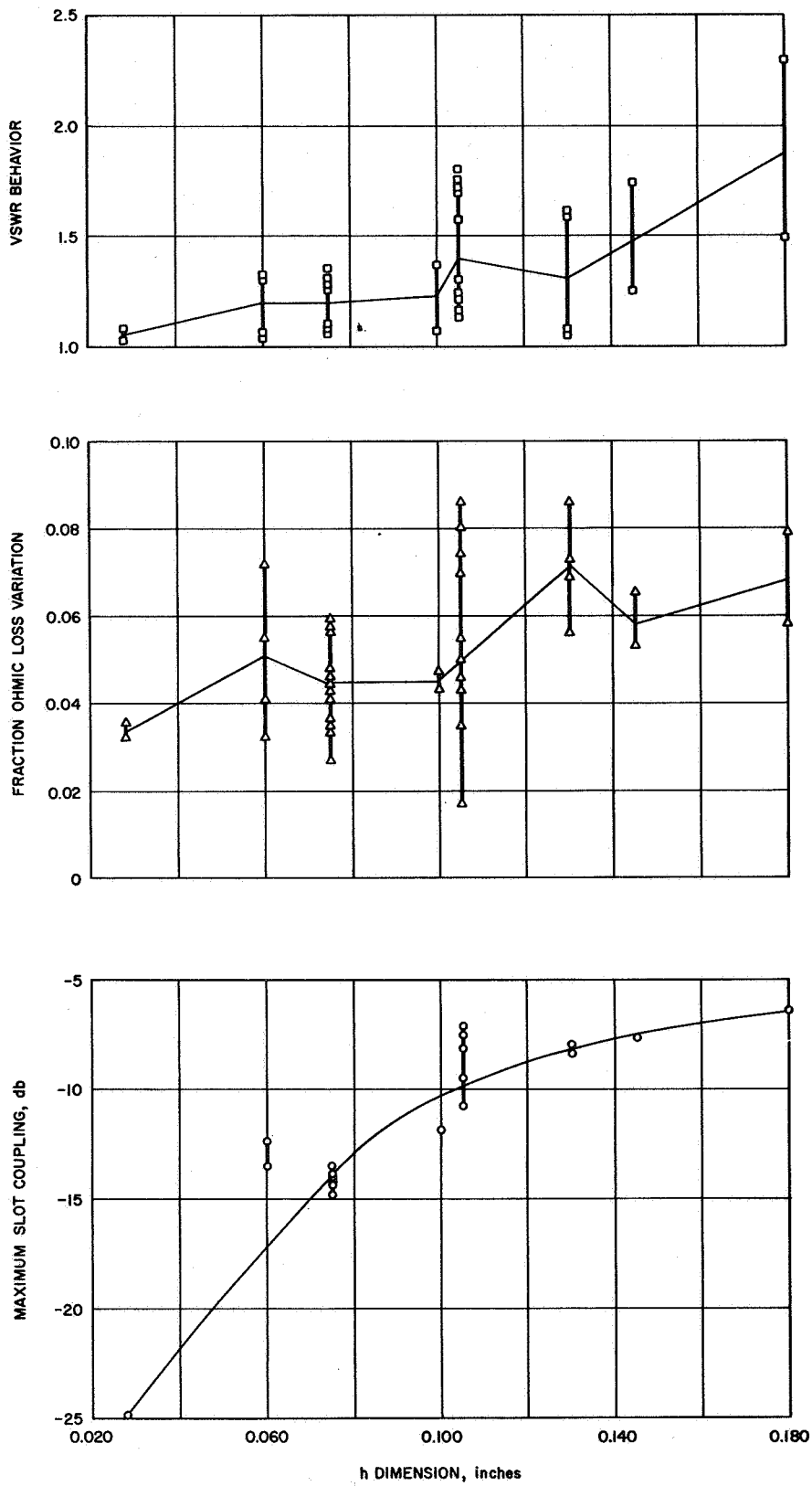


Figure 5. Coupling, loss, and VSWR response versus  $\underline{h}$  parameter for a 2-diode iris unit.

To improve the repeatability of the iris units, each diode was secured to the waveguide broadwall containing the slot by a vertical post soldered in place (see Figures 6 and 14). The post had a diameter of 0.050 inch and a length sufficient to accommodate the needed  $h$  dimension. A 0.020-inch hole, located at the appropriate  $h$  dimension along the post, was drilled and used to snug-fit the diode lead wire to the post.

R-f power handling measurements were performed on 6-volt and 40-volt varactor diodes in a two-diode iris configuration with  $h = 0.130$  inch and  $d = 0.290$  inch. These consisted of taking coupling and ohmic loss readings as a function of bias voltage because it was not evident which diode characteristic would be most sensitive to r-f power level. Data for the 6-volt diodes are shown in Figures 7 and 8 for four different r-f power levels. The 6-volt diodes began to rectify above 0.1 milliwatt. At these power levels they simultaneously exhibited non-monotonic coupling behavior (Figure 7) and increased ohmic loss (Figure 8). Corresponding coupling and ohmic loss behavior for the 40-volt diodes is shown in Figures 9 and 10, respectively. Here at a one milliwatt power level the maximum coupling value was about -7 db and the ohmic loss varied from 11 to 27 percent. At higher power levels the ohmic loss nearly uniformly and progressively increased, but the coupling variation remained monotonic. The drive power for the 40-volt diodes was on the order of milliwatts.

### 2.1.2 Four-Diode Iris Configurations

A trade-off design for a four-diode iris was chosen from the curves in Figure 5 of two-diode iris amplitude and loss characteristics versus  $h$  parameter. It was anticipated that this design would provide, within  $0.140 \geq h$  (inches)  $\geq 0.100$ , a maximum coupling of at least -10 db (which corresponds to a normalized conductance of 0.10) with 360 degrees of phase control and a nominal ohmic loss of 10 percent (i. e., 0.46 db dissipative insertion loss). These values represented a 5-db increase in amplitude control for complete phase control and a 65-percent reduction in ohmic loss when compared with earlier four-diode iris designs.<sup>2</sup>

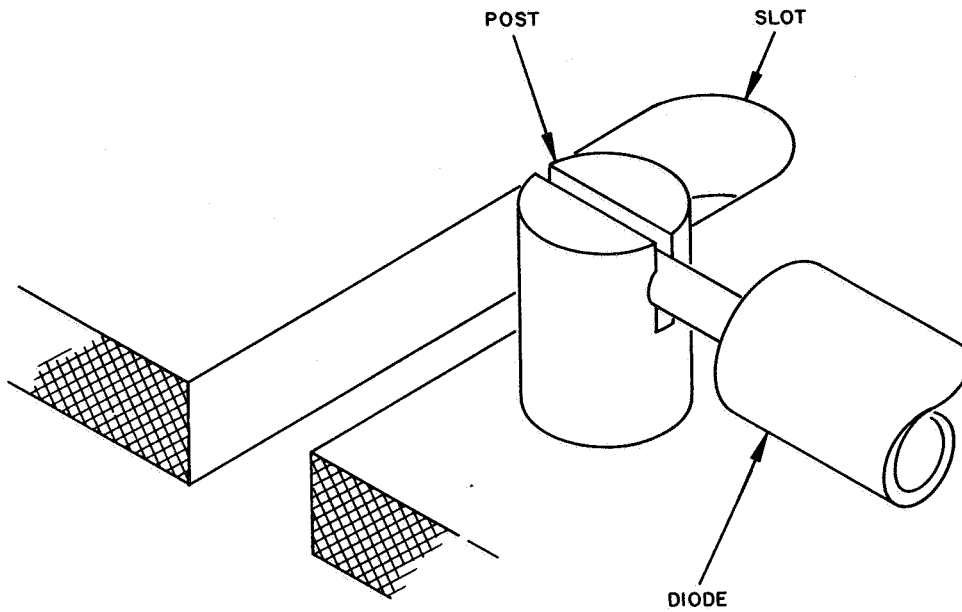


Figure 6. Construction of post used to fasten diode near slot.

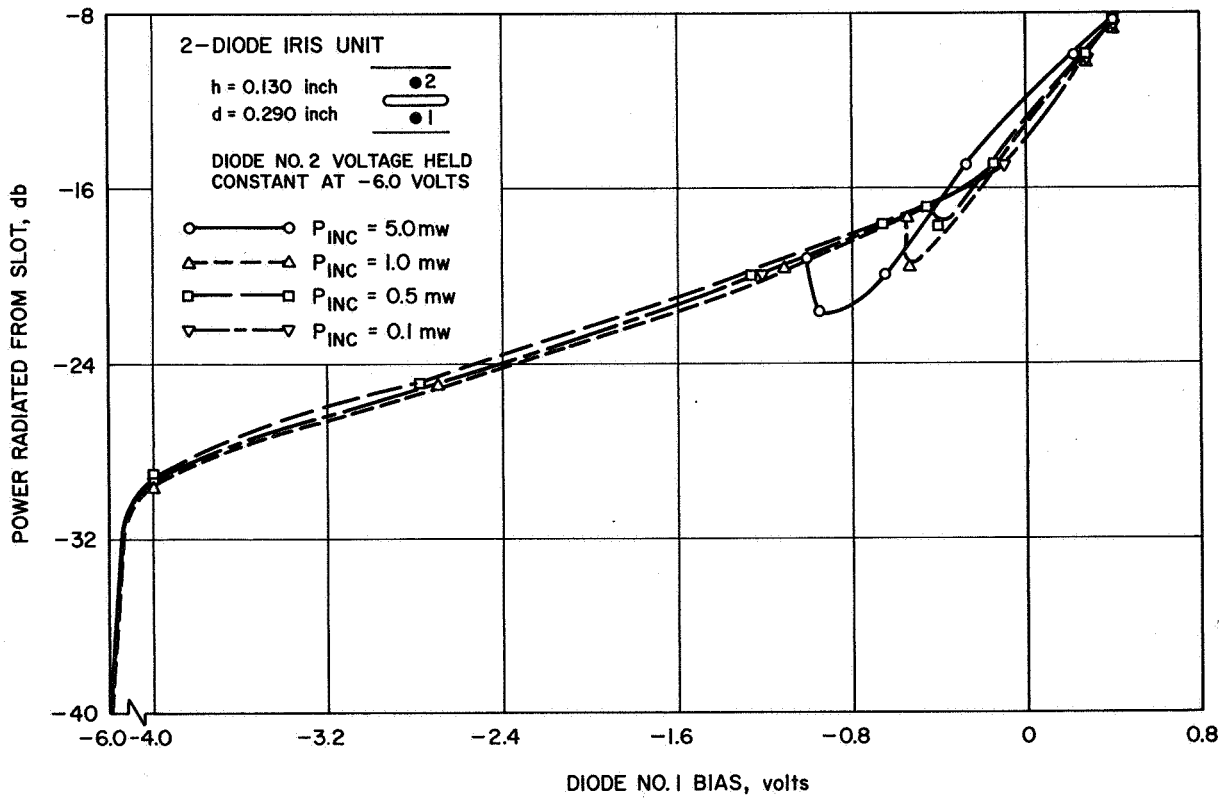


Figure 7. Effect of r-f power level on slot coupling for 6-volt diodes.

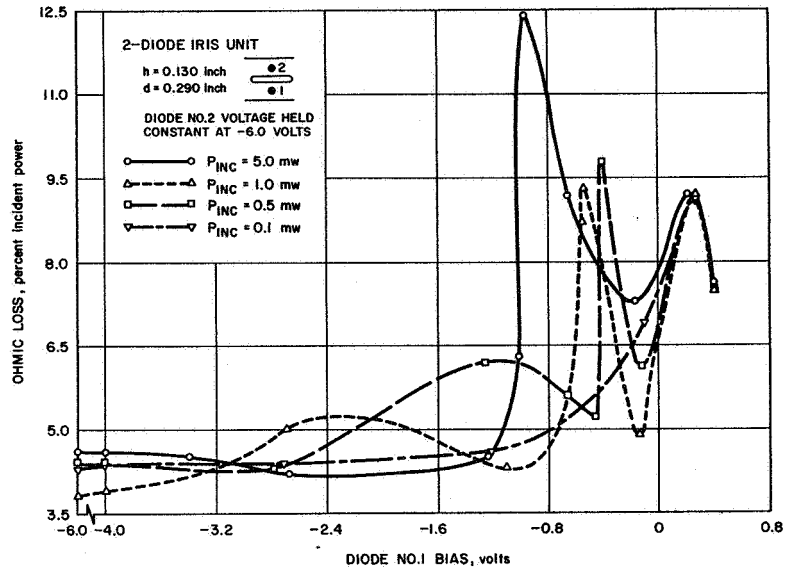


Figure 8. Effect of r-f power level on iris ohmic loss for 6-volt diodes.

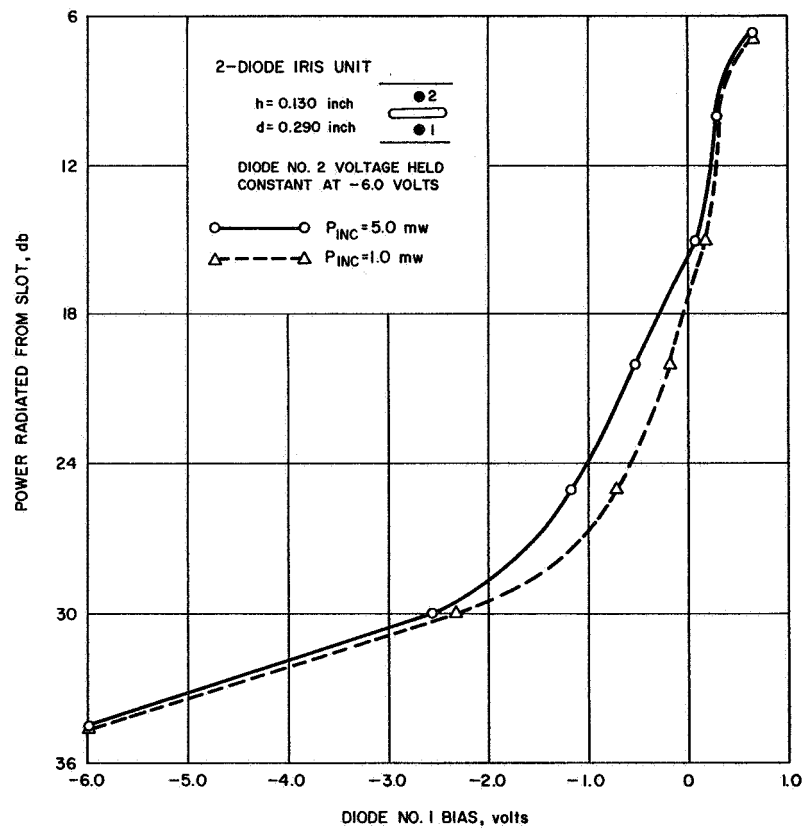


Figure 9. Effect of r-f power level on slot coupling for 40-volt diodes.

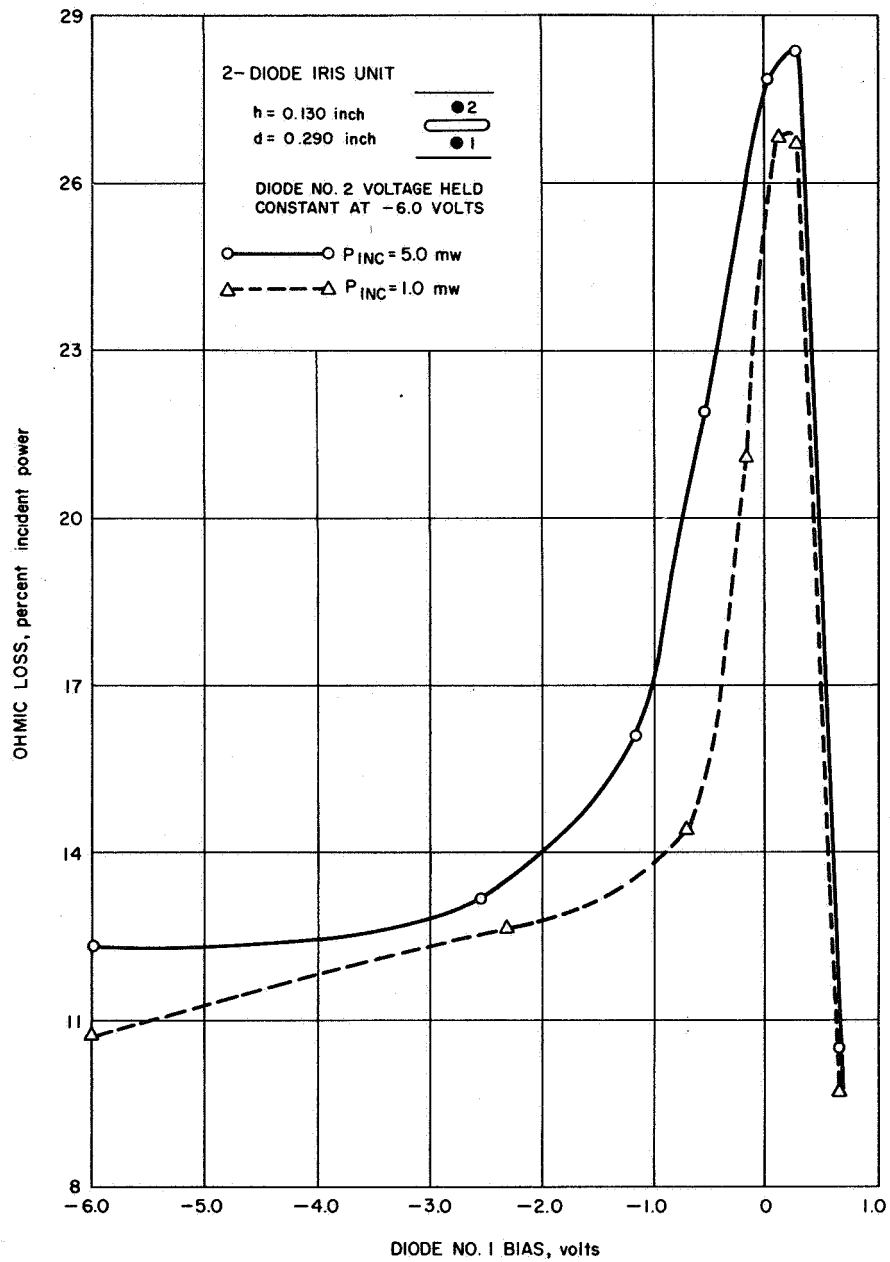


Figure 10. Effect of r-f power level on iris ohmic loss for 40-volt diodes.

Three four-diode iris configurations were designed, fabricated, and tested. Each configuration contained two identical two-diode irises displaced  $D$  equal an eighth guide wavelength in either direction from the slot center. Two units used  $h = 0.105$  inch with one unit having a 0.030-inch slot offset as a check on previous results and the other unit having the slot on the centerline. The third unit used  $h = 0.130$  inch and no offset. A modified amplitude measuring setup, which included a precision phase shifter in the slot radiation arm, was used as a phase bridge (Figure 11). Table II lists the initial data taken for these units. The third unit displayed a maximum coupling of -7.8 db which was over 3 db greater than the other units and a tolerable VSWR variation. Further measurements of slot phase control and iris ohmic loss were therefore confined to this unit.

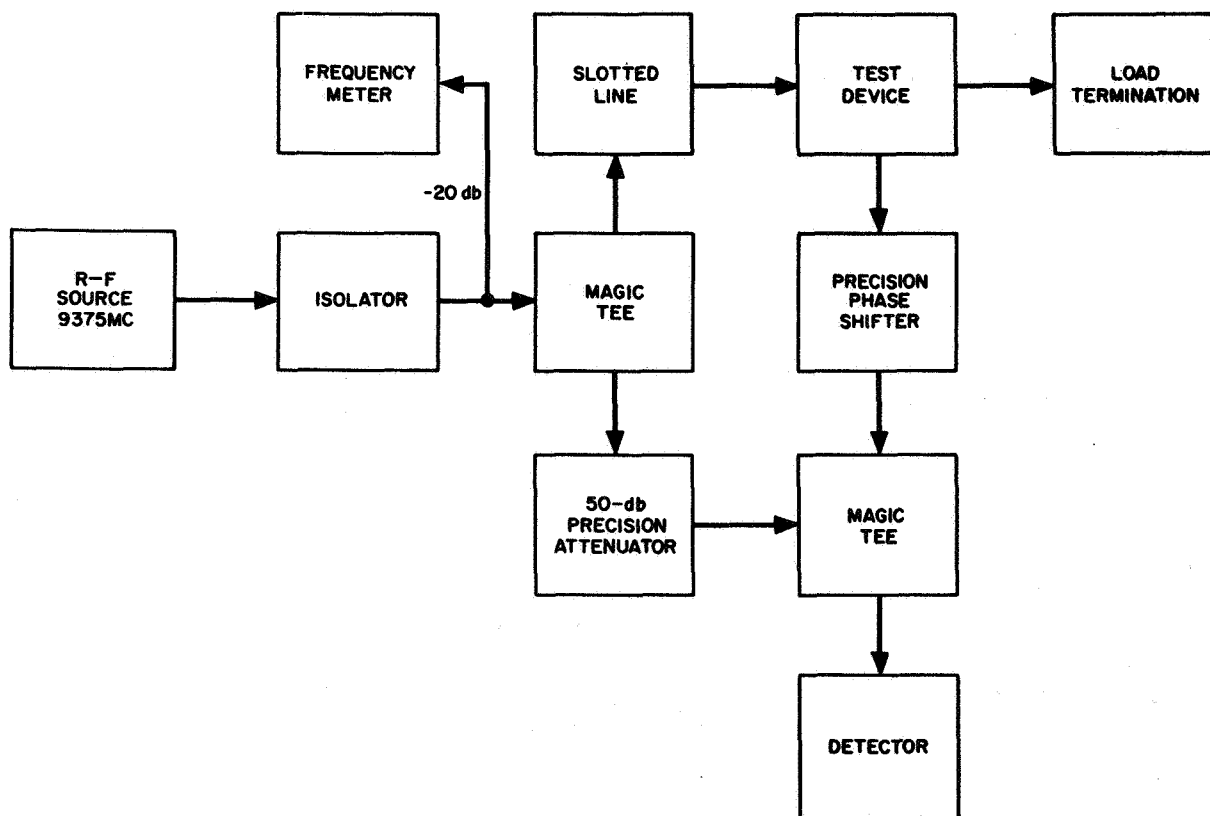


Figure 11. Phase bridge circuit block diagram.

<u>h</u> Parameter (inches)	Maximum Amplitude Control (db)	VSWR Variation	Additional Remarks
0.105	-11.0	1.06 - 1.26	0.030 inch slot offset
0.105	-12.0	1.07 - 1.16	No offset
0.130	- 7.8	1.05 - 1.65	No offset

Table II. Coupling and reflection behavior of three four-diode iris configurations.

An extensive polar plot of the amplitude and phase of slot radiation was recorded as shown in Figure 12. The amplitude is plotted radially with zero radiation located at the origin, and the phase is plotted as the polar angle. The unit provided 360 degrees of phase control at amplitude levels up to about -14 db and reduced phase control ranges for greater amplitude values; the maximum coupling was -7.8 db at a phase angle of 54 degrees or 240 degrees. Ohmic loss measurements revealed a pronounced resonance effect for the unit (see depiction in Figure 13). Measurements performed at three distinct coupling levels and plotted as a function of slot phase angle showed the loss to increase progressively with increased coupling and to achieve peak value at a slot phase angle of 160 degrees; maximum loss was 16.1 percent at the -14 db slot coupling level. Interchanging the diodes on opposite sides of the slot shifted the resonance point by 180 degrees to a slot phase angle of 340 degrees. Replacing all diodes reduced the peak loss to 13.2 percent. The VSWR response of the unit varied from 1.05:1 to 1.60:1.

A tuner suitably adjusted in the slot coupling arm of the test unit was shown to provide 360 degrees of phase control at a slot coupling level of -7.5 db; the corresponding VSWR variation extended from 1.28:1 to 2.14:1. This result with the tuner stimulated a series of revisions in the geometrical design of the unit in an attempt to duplicate the results without the tuner. The many types of design revisions that

were empirically investigated included variations in the slot length, the use beneath the slot of steps of various heights, lengths, and overall shapes, the use of horizontally-oriented septa of different lengths and positions relative to the slot, and variations in both the transverse operation  $d$  between diodes and the longitudinal separation  $D$  between pairs of diodes. All measurements were taken with the slot waveguide arm of the test fixture removed, a detecting horn placed over the slot, and the phase bridge setup calibrated to measure the amplitude and phase of the slot radiating into free space.

None of the revised configurations succeeded in achieving the performance of the unit with a tuner, but the overall performance of one configuration made it suitable for use in an array (see following section 2.1.3). The design of this unit (Figure 14) contained  $h = 0.130$  inch,  $d = D = 0.290$  inch, and a slot length of 0.540 inch. It provided 360 degrees of phase control up to a coupling level of -14.5 db; the VSWR varied from 1.13:1 to 1.55:1 and the average ohmic loss varied from 14.5 percent (0.67 db insertion loss) at high coupling values to 8.1 percent (0.36 db) at low coupling values. These results represented a negligible increase in slot coupling control over previous four-diode iris designs, but a 49-percent reduction in nominal ohmic loss.

### 2.1.3 Five-Element Array

To illustrate the reduction in four-diode iris ohmic loss and to demonstrate electronic beam scanning, a traveling-wave linear array containing five radiating slots with a 4-diode iris control unit at each slot was designed and fabricated (Figure 15). The diode iris unit used was the most promising of the revised configurations described in the preceding section. End-feeding and an inter-element spacing of a half-free-space wavelength were used in the array design, and the diode irises were adjusted to always generate a uniformly illuminated aperture over a scan range of  $\pm 60$  degrees.

With the array not radiating, the measured insertion loss with and without the diodes revealed the average four-diode iris to have an ohmic loss of 0.39 db. With the aperture adjusted for uniform,



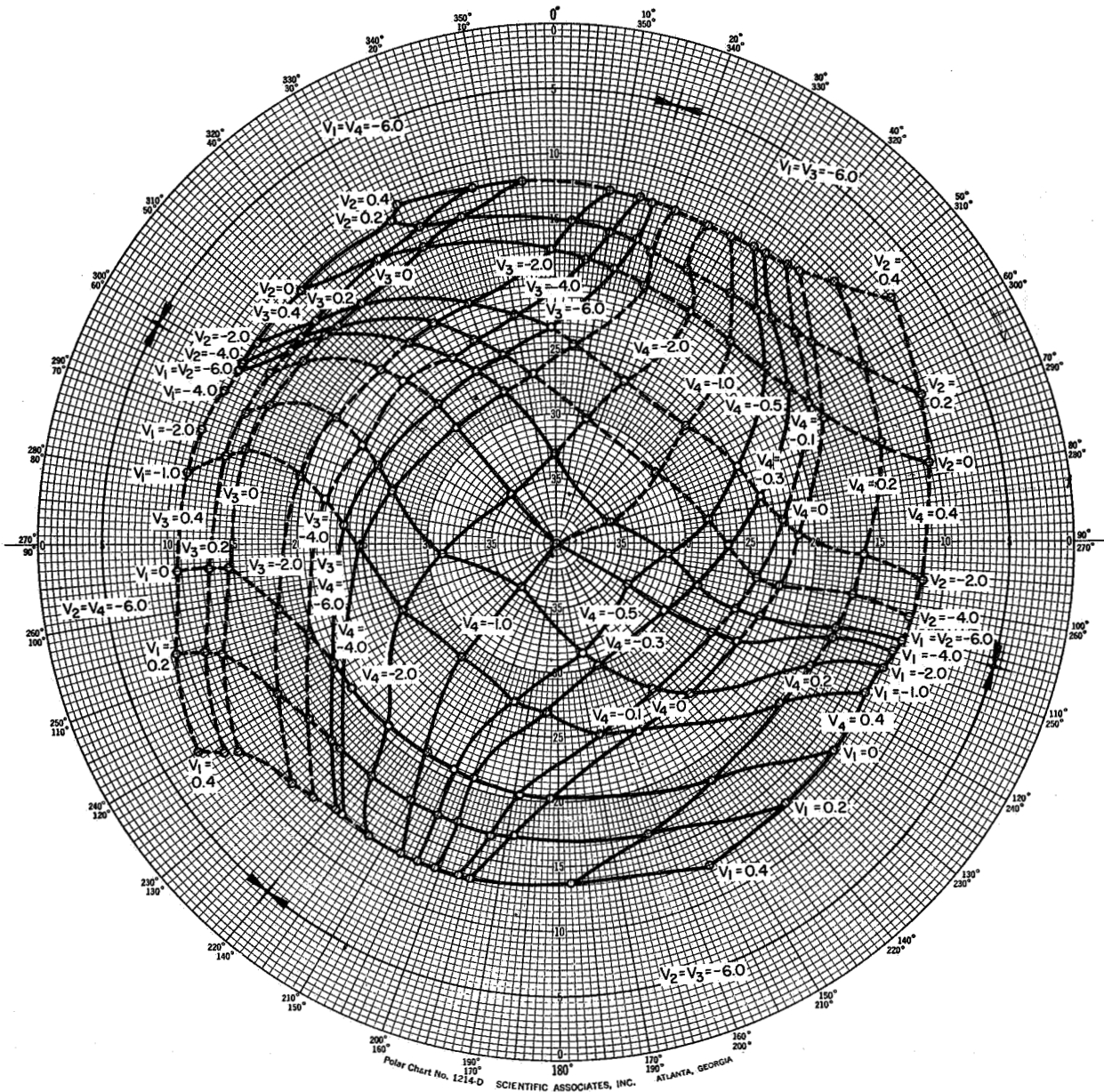


Figure 12. Phase and amplitude variation of a 4-diode iris controlled slot radiator.

$$d = 0.290 \text{ inch}$$

$$D = 0.440 \text{ inch}$$

$$h = 0.130 \text{ inch}$$

$$f = 9.375 \text{ Gc}$$

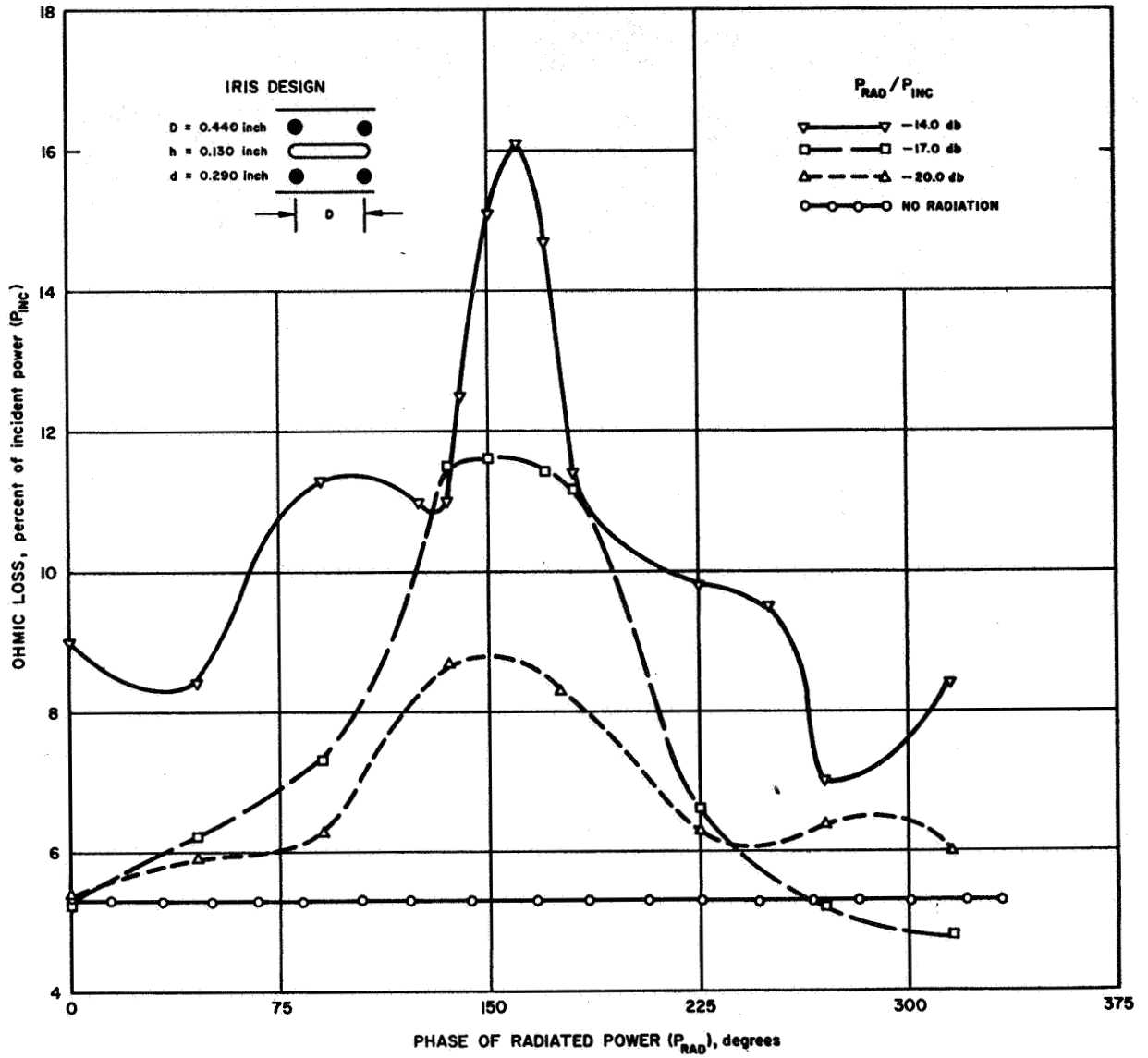
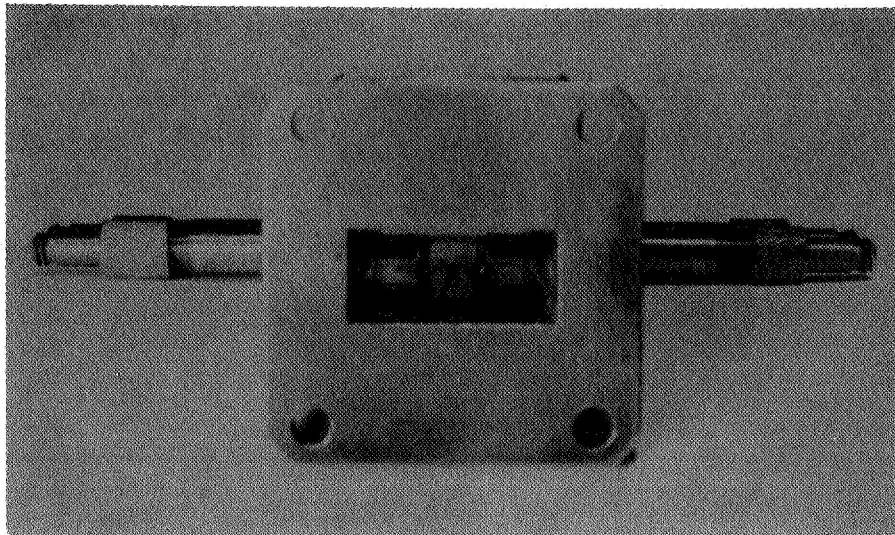
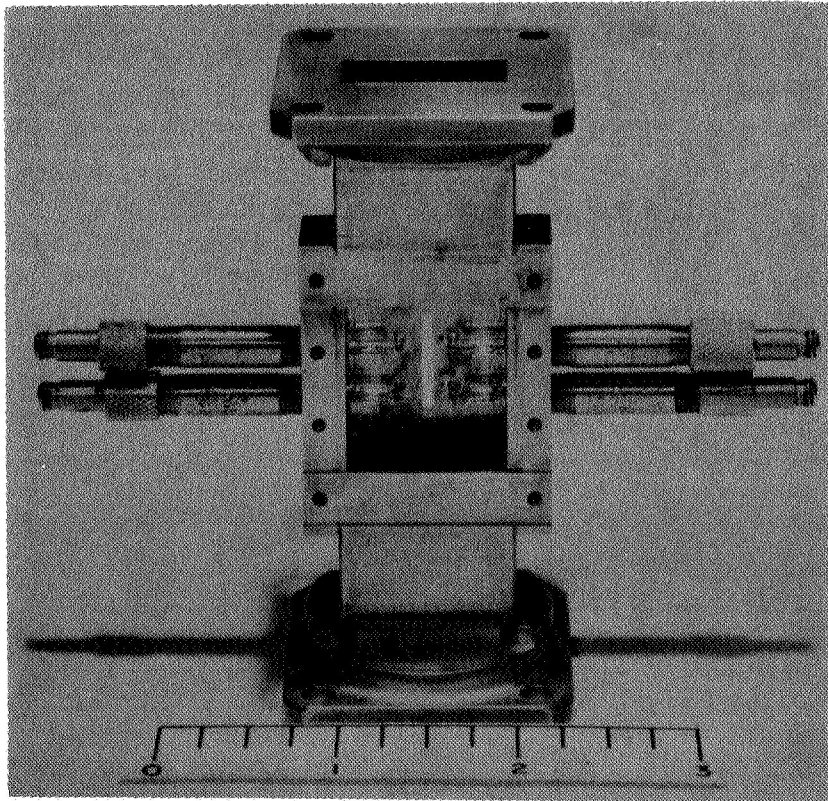


Figure 13. Loss resonance effect in 4-diode iris design.



a. End view



b. Bottom view

Figure 14. A 4-diode iris controlled slot radiator.

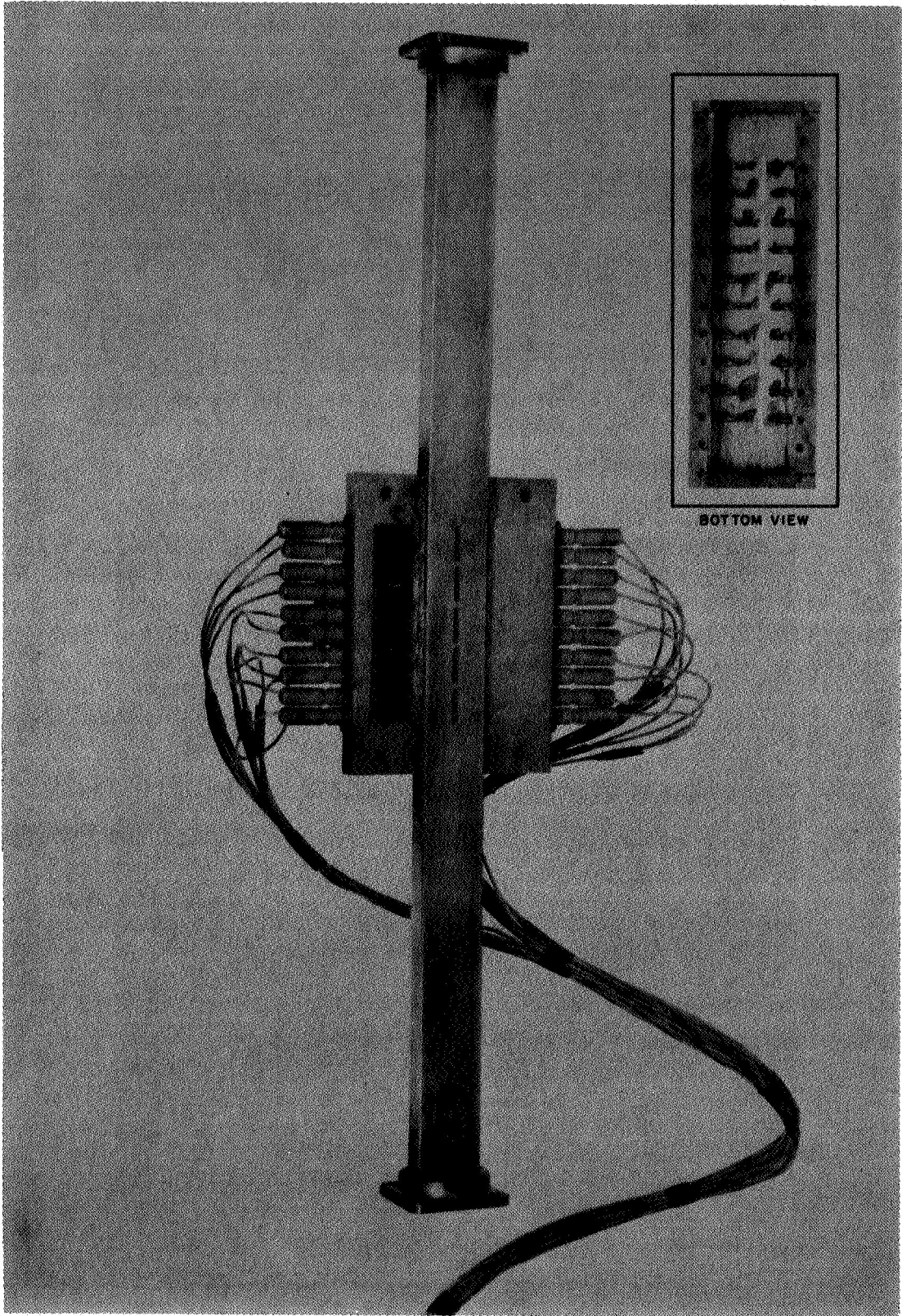


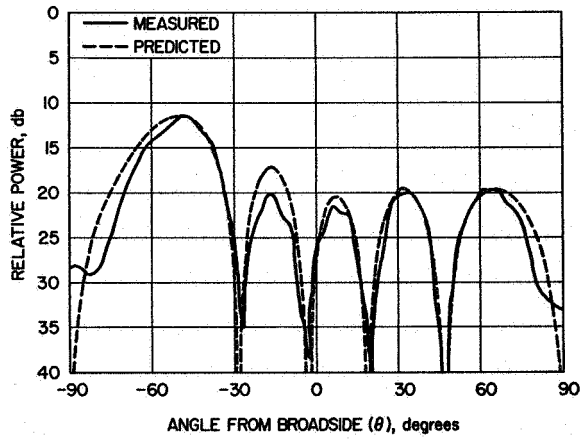
Figure 15. Five-element diode-iris array.

broadside radiation, the average ohmic loss became 0.37 db. Both loss figures lie within those predicted from the single four-diode iris results with the latter figure representing a 71 percent reduction in ohmic loss when compared with earlier, single four-diode iris units.<sup>2</sup>

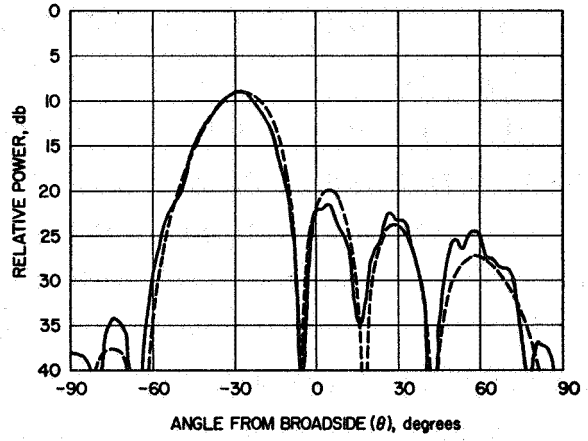
Electronic beam scanning was demonstrated by the generation of five distinct beams over the 120-degree scan range. Relative inter-element phase differences of  $0^\circ$ ,  $\pm 90^\circ$ , and  $\pm 156^\circ$  were established in the aperture to produce beams at  $0^\circ$ ,  $\pm 30^\circ$ , and  $\pm 60^\circ$  from broadside. Each phasing condition was established by sampling the radiated fields from the individual plots with a slot probe in conjunction with a phase bridge. In Figure 16 measured array patterns are compared with those predicted from the measured slot excitation. Generally good agreement in beam pointing direction and sidelobe structure exists. In the patterns for the  $\pm 30^\circ$  and  $\pm 60^\circ$  beams, it should be noted that the reduction in beam scan angle has been caused by the H-plane patterns of the slot elements.

## 2.2 PLASMA IRIS FEASIBILITY INVESTIGATION

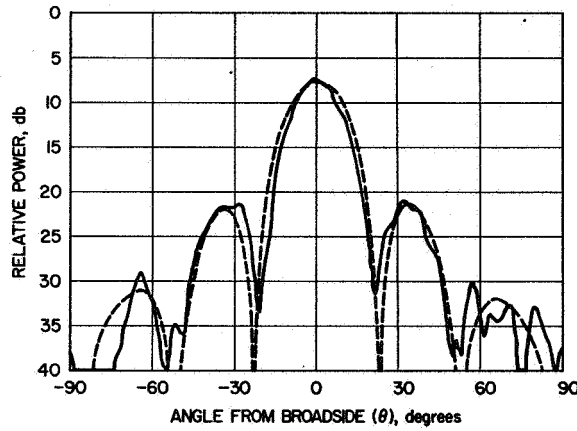
Plasma studies were initiated to devise a plasma iris design which would be capable of operating at high r-f power levels (on the order of 100 watts) and which would introduce lower r-f loss than its semiconductor counterpart. With the assistance of the Plasma Physics Department of Hughes Research Laboratories, Malibu, three different plasma varactor iris designs were investigated, two as part of the NASA/Langley studies and one as an internal research project of the Hughes Aircraft Company. These designs were the plasma microdiode, the positive column plasma reactance tube, and the electron injection plasma varactor. Analyses were made to predict plasma varactor performance, and experiments were conducted to corroborate the feasibility of using a plasma iris design.



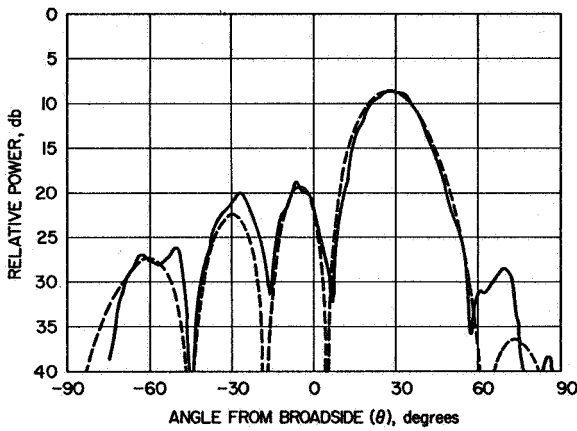
a. phased for  $\theta = -60^\circ$



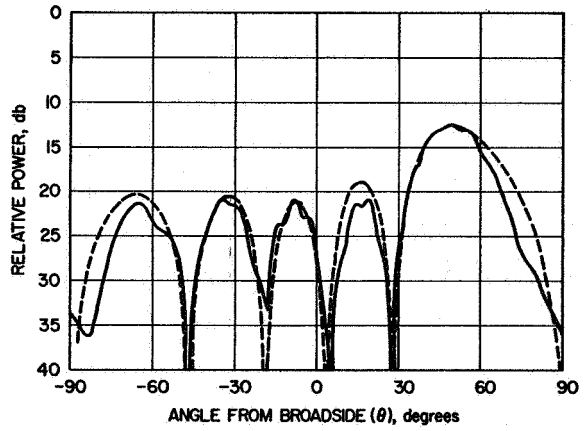
b. phased for  $\theta = -30^\circ$



c. phased for  $\theta = 0^\circ$



d. phased for  $\theta = +30^\circ$



e. phased for  $\theta = +60^\circ$

Figure 16. Radiation patterns of 5-element array illustrating 120 degrees of electronic beam scanning by 4-diode iris control.

### 2.2.1 Theory of Plasma Varactors in Waveguides

A plasma varactor iris in a waveguide, in first approximation, is a column of dielectric whose complex dielectric constant is equal to that of the plasma and is therefore given by<sup>5</sup>

$$\epsilon = \epsilon_0 \left[ 1 - \frac{\omega_p^2}{\omega(\omega + j\nu)} \right] \quad (1)$$

where

$$\omega_p = 2\pi f_p$$

$$f_p = \sqrt{\frac{e^2 n_-}{\epsilon_0 m_-}} = \text{electron plasma frequency}$$

$n_-$  = electron density

$m_-$  = electron mass

$\nu$  = electron collision frequency

In the present considerations and in the application of Equation (1), dielectric losses of the glass walls will be neglected. Furthermore, the r-f electric field is assumed to be parallel to the axis of the plasma column.

For experimental evaluation of the effectiveness of a plasma varactor in a waveguide, the plasma varactor is located at a plane of voltage standing wave maximum (open circuit plane) in a short-circuited waveguide. As the plasma density increases, the dielectric constant decreases, as shown in (1). This relation means that the r-f electric field tends to be excluded from the plasma region, or in terms of equivalent circuit, that the waveguide is loaded by a shunt inductance. The maximum possible phase shift of the standing wave pattern between the signal generator and the plasma varactor will be produced when the

electric field is entirely excluded from the plasma, which happens when  $\omega_p \gg \omega$  and  $\epsilon \rightarrow -\infty$ . This condition is equivalent to a vanishingly small shunt inductance, which is a short circuit. Under these conditions the plane of the plasma varactor, which was an open circuit plane in the absence of plasma, becomes a short circuit plane. The result is a 90-degree phase shift ( $\Delta\Phi = 90^\circ$ ) of the standing wave pattern in the waveguide. For practical geometrical configurations (plasma column diameter  $\cong 15$  percent of waveguide width and located in region of maximum r-f electric field), this  $90^\circ$  phase shift is closely approached as soon as  $\epsilon$  becomes negative. From (1) (with  $\nu < \omega$ ), this condition is seen to be satisfied when

$$\omega_p \cong \omega \quad (2)$$

It therefore follows that to achieve a phase shift on the order of  $90^\circ$  by means of a plasma varactor in a waveguide, the plasma frequency in the tube has to be varied between zero (or  $\omega_p \ll \omega$ ) and the value given in (2). It should be noted that  $\omega_p \propto \sqrt{n_-}$ . For X-band this variation means that

$$0 < n_- \leq 10^{12} \text{ electrons/cm}^3 \quad (3)$$

It remains to be determined if a phase shift of  $90^\circ$  under the measuring conditions described above corresponds to a sufficient reactance variation for the control of the slot current in a slot antenna array. To answer this question, it is sufficient to measure under the same conditions the phase shift produced by a reactance variation known to be sufficient to produce the desired slot current control. Such measurements have been performed with semiconductor varactors and have shown that a phase shift of  $45^\circ$  is in fact sufficient.

The conclusion drawn from these considerations is that the plasma density required for an X-band plasma varactor is determined by the conditions of (3).



Quality Factor Q. To determine the quality factor Q of a plasma varactor, it is necessary to take into account not only the volume losses within the plasma, but also the r-f losses caused by the r-f kinetic energy carried out of the interaction space by electrons leaving this space. The total Q of the plasma varactor can therefore be separated into two parts:

$$\frac{1}{Q} = \frac{1}{Q_v} + \frac{1}{Q_s} \quad (4)$$

where  $Q_v$  is the "volume Q" and takes the volume losses into account, while  $Q_s$  is defined as the "surface Q" and takes into account the losses due to the transport of r-f. electron kinetic energy out of the interaction space.

It can be shown that<sup>3</sup>

$$Q_v = \frac{\omega}{\nu}$$

$$Q_s \approx \frac{\omega l}{\bar{v}_z}$$

where

$l$  is the waveguide height

$\bar{v}_z$  is the mean axial electron drift velocity along the column

When  $\omega = 2\pi \cdot 10^{10}$ ,  $l = 1$  cm, and  $\bar{v}_z = 10^8$  cm/sec, the surface Q becomes

$$Q_s \approx 600$$

This value is much greater than the highest realizable values for  $Q_v$  calculated for the most favorable discharge configurations. For this reason the surface losses will henceforth be neglected, and the Q will be evaluated by the relation

$$Q \approx Q_v \approx \frac{\omega}{\nu} \quad (5)$$

### 2.2.2 Cold Cathode Microdiode Design

A cold cathode design was the first design considered in this investigation because its compact package size would permit it to be readily interchangeable with a Hughes semiconductor diode. This tube device, shown in Figure 17, consisted of a voltage (or current) controlled plasma which was contained by a glass envelope and two metal electrodes. The term "cold cathode" applies because the cathode was designed to operate without a heating filament. Since tube designs of this type were not available commercially, various models were fabricated in the laboratory and tested for evaluation; each one was characterized by a specially prepared emissive cathode surface coating. Coatings of aluminum, aluminum oxide, and barium oxide on nickel were tried and shown to provide current-voltage characteristics adequate for preliminary experimentation; barium oxide material yielded the highest plasma densities because it ejected the highest number of electrons.

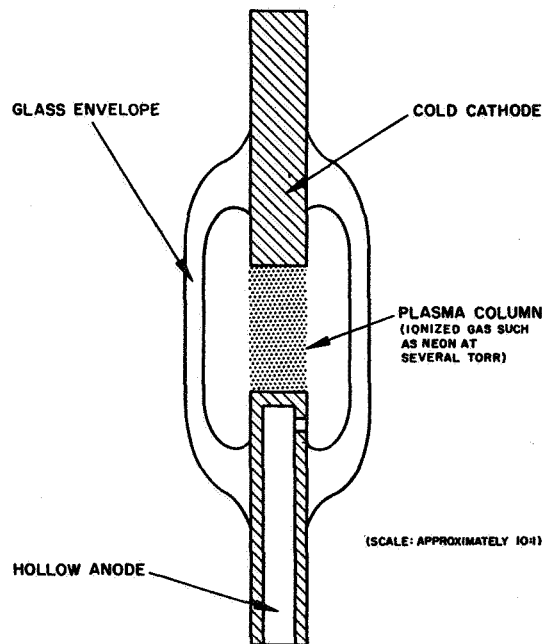


Figure 17. Plasma microdiode design.

Initially, admittance measurements were performed on the microdiode tube to determine its variable reactance behavior. Measurements of each tube were made with the tube vertically positioned at the centerline of the broadwall of an X-band rectangular waveguide, a quarter guide wavelength in front of an adjustable short circuit. The tube was considered as a lumped element in shunt with the equivalent transmission line circuit. The admittance measuring setup included a vacuum pump system which was attached directly to the plasma tube and which facilitated the injection or evacuation of various gas mixtures at various pressures. The first tube tested contained an aluminum cathode and utilized either air or neon gases at pressures ranging from 10 to 25 Torr (1 Torr = 1 millimeter mercury pressure). Air at 15 Torr produced a maximum phase shift in the standing wave pattern of 3 degrees; this response required a 320 volt bias and 50 milliamperes of current and indicated insufficient plasma density. A second microdiode design, fabricated with a barium oxide coating on a nickel cathode and containing neon gas at 15 Torr, produced a standing wave pattern shift which corresponded to a 104 degree change in phase of the reflection coefficient; it also required up to 340 volts of bias and 50 milliamperes of current to operate and exhibited a one-way transmission loss which varied from 31 to 47 percent (one-way transmission loss in percent =  $50(1 - |\Gamma|^2)$  where  $|\Gamma|$  is the magnitude of the reflection coefficient). The phase shift is depicted on a Smith Chart in Figure 18 on which the performances of a Hughes semiconductor diode and a positive column reactance tube have been plotted for comparison.

The high insertion loss and discharge power needed for the cold cathode design and the anticipated problems of heat dissipation, impedance matching, and r-f choke construction discouraged further work with this type of design.

### 2.2.3 Positive Column Plasma Reactance Tube

Another design studied was a plasma column (glass enclosed) with two electrodes external to the waveguide. The tube used was a Bendix

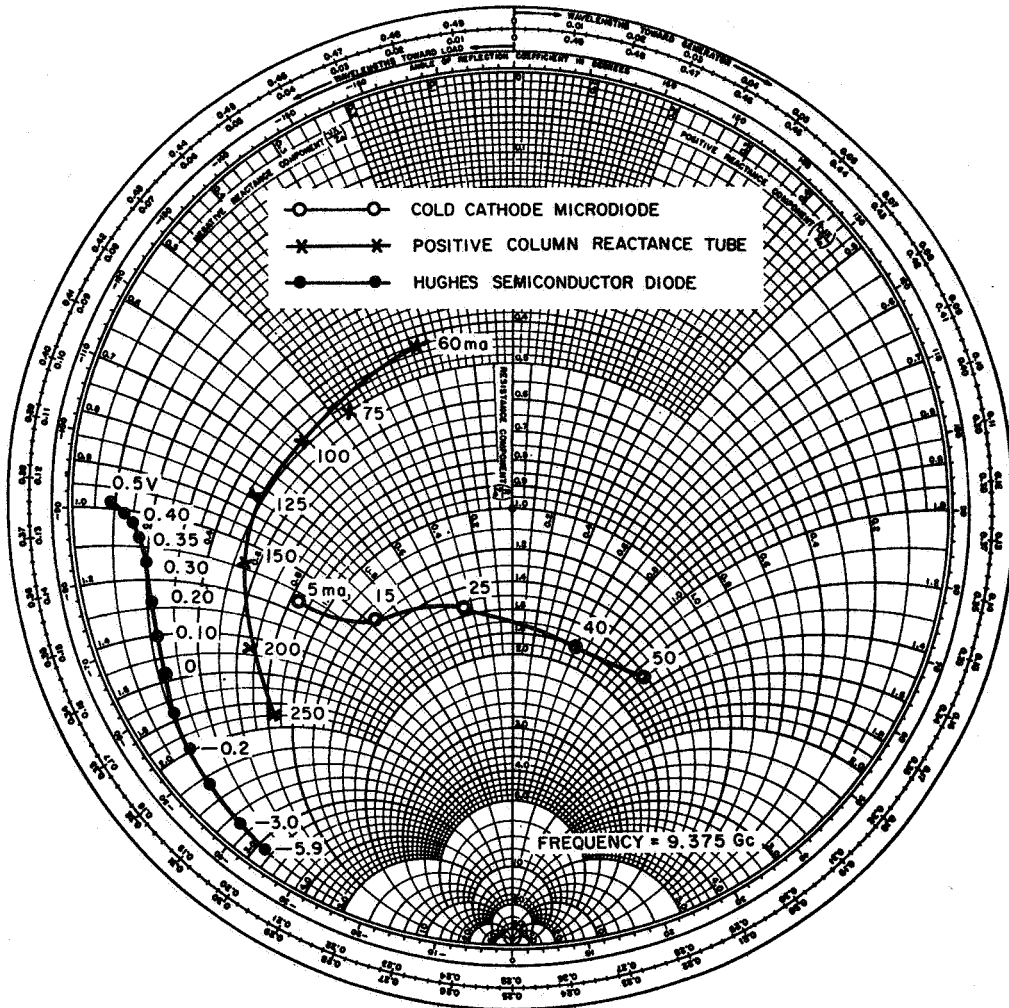


Figure 18. R-f admittance characteristics of semiconductor and plasma varactors.

Model TD-41, which is similar to the TD-42 Model shown in Figure 19. The Model TD-41 tube had an interelectrode spacing of 6.25 inches and an inner diameter of 5 millimeters; it contained argon gas at a pressure of approximately 20 to 30 Torr. The tube exhibited a 100-degree phase change in its admittance plot (see Figure 18) and a one-way transmission loss that varied from 24.4 to 40.6 percent. Operating as a cold cathode discharge device, the tube drew 60 to 250 milliamperes of current and required a discharge power of 10 to 32 watts. Three hot cathode tube designs with inner diameters of 2, 3, and 5 millimeters were also fabricated and tested. Their designs represented modified Bendix tube

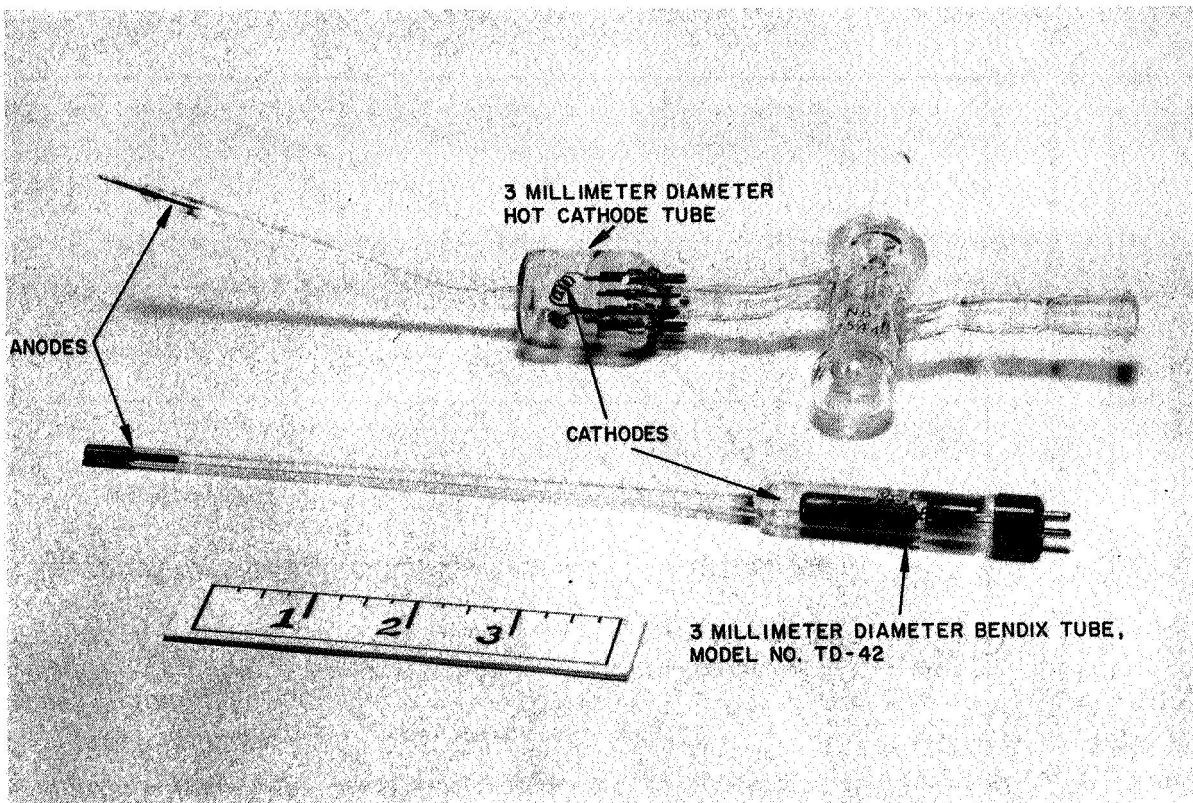
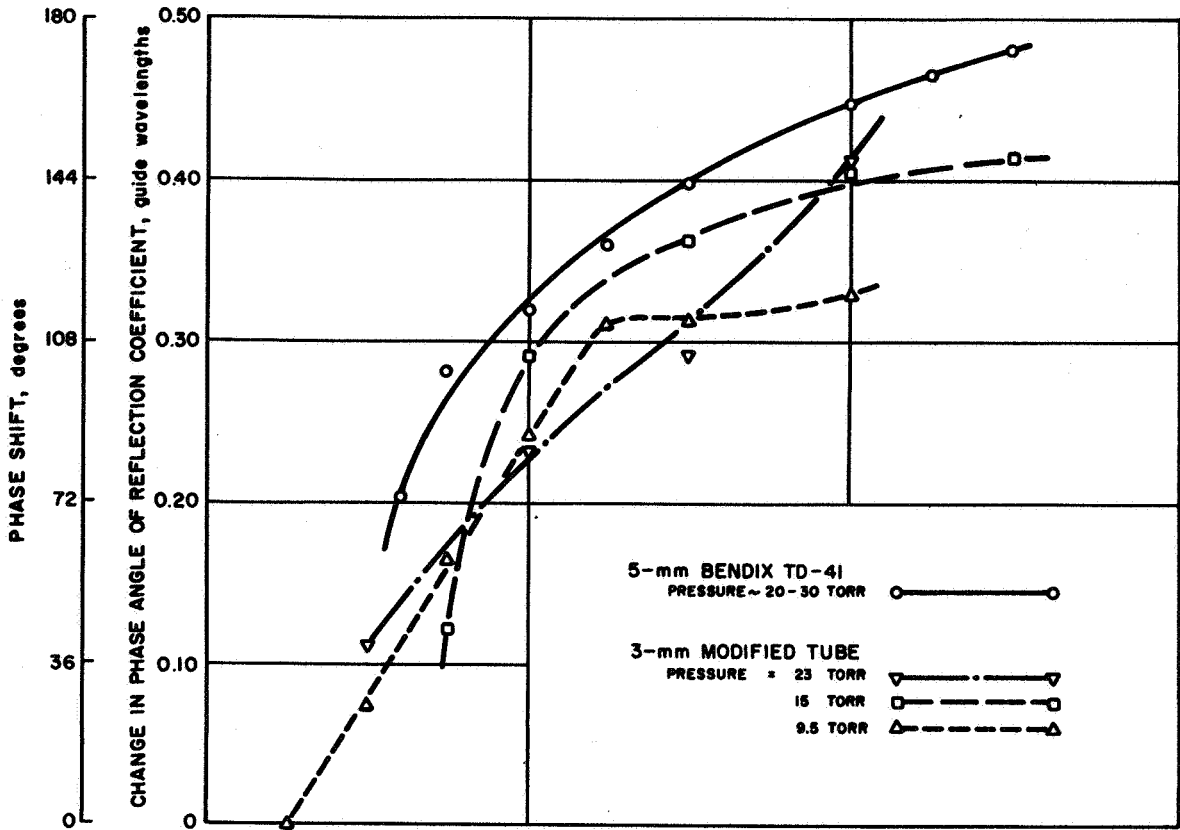


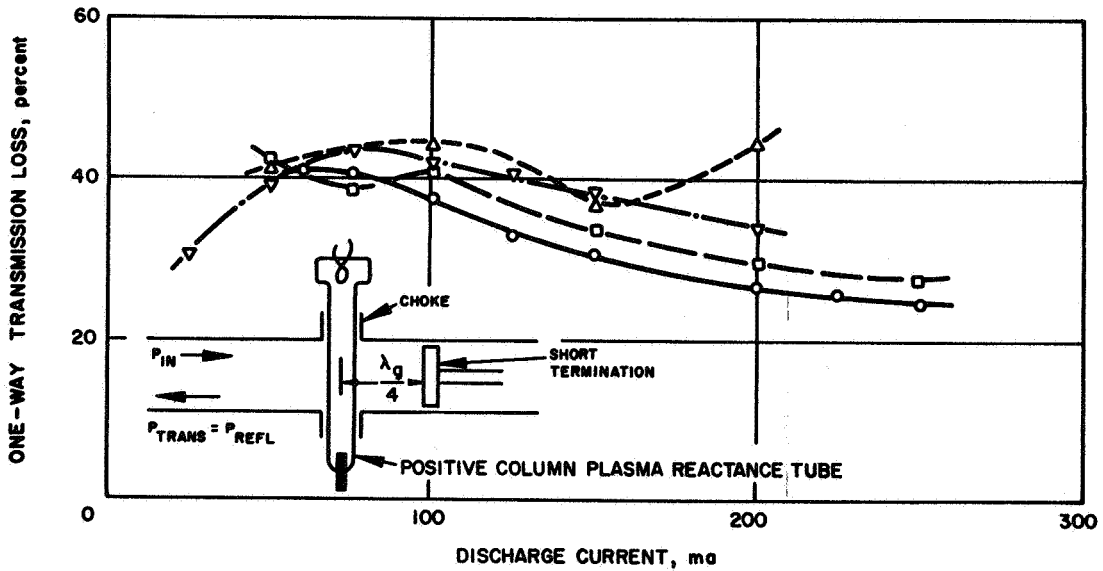
Figure 19. Positive column plasma reactance tubes.

designs in which a barium oxide-coated spiral winding was used as a hot cathode filament. The tubes were used to determine the influence of the tube diameter, type of gas, and gas pressure on the varactor performance in the waveguide. As expected the tube design resulted in current-voltage discharge characteristics which were typically the same as those for the Bendix TD-41 tube: 300 to 400 volts of applied voltage and 50 to 250 milliamperes of current flow. The best results were obtained using a 3-millimeter tube containing argon gas at a pressure of 15 Torr; this tube exhibited 97.2 degrees of phase change and a one-way transmission loss of 27.7 to 42.1 percent. These and other similar data at different gas pressures in the 3 millimeter tube are compared in Figure 20 with the results for the commercial Bendix tube TD-41. Not shown are the data recorded using xenon and krypton gas which essentially displayed the same microwave performance.

Plasma instability occurred in tubes of this type over the pressure range measured. A photo-detector diode connected to an



a. phase shift.



b. one-way transmission loss.

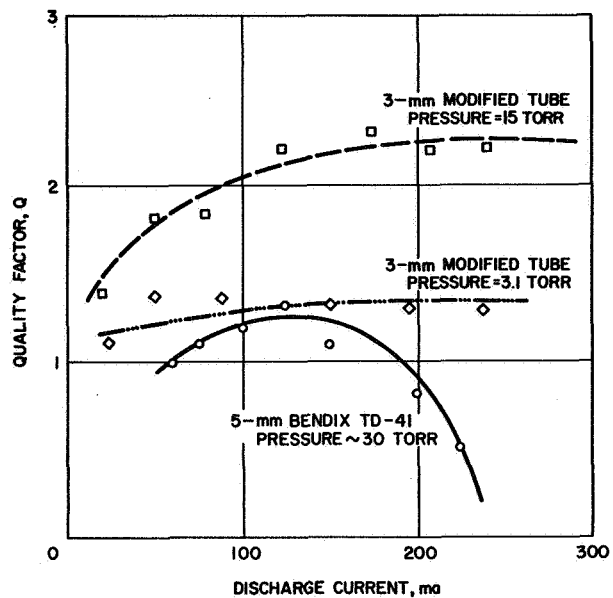
Figure 20. Measured electrical characteristics of positive column plasma reactance tubes.

oscilloscope displayed up to 70-percent modulation of the plasma density. Since the period of oscillation was 10 microseconds, response reading that were observed on the microwave detecting equipment corresponded to average states of plasma density.

Measured Q. The experimental value of Q as a function of discharge current was obtained from the phase shift and SWR measurements shown in Figure 20. By transformation of these results, the imaginary and real part of the impedance presented by the plasma to the waveguide was obtained. From (5) the ratio of imaginary to real part of this impedance is equal to the Q of the plasma reactance and is shown in Figure 21. It is observed that for pressures between 3 and 15 Torr, the measured Q is  $1 < Q_{\text{meas.}} < 2.5$ .

The measurement of the somewhat higher Q at 15 Torr than at 3 Torr can be understood as a consequence of the Ramsauer effect. The mean electron energy at 3 Torr being higher than at 15 Torr, the electron-atom collision cross-section will be higher at 3 Torr (Ramsauer effect); this increased collision cross-section can make  $P_c$  increase faster than the inverse of the pressure p. The result is that the collision frequency can in fact increase as the pressure

Figure 21. Quality factor Q versus discharge power for positive column plasma reactance tubes.



decreases. As the pressure is further decreased (e. g., below 3 Torr), this anomaly will not prevail anymore, and the collision frequency is expected to decrease. The phase shift measurements of Figure 20(a) show, however, as was also theoretically expected, that this discharge current needed to obtain a sufficient phase shift at pressures below 3 Torr becomes impractically high. Furthermore, striations at lower pressure make SWR and Q measurements rather difficult. For these reasons, no data of SWR and Q are shown for  $p < 3$  Torr with the positive column tubes.

Discharge power. The power dissipated in the discharge for tubes which yielded the measurements of Figures 20 and 21 is shown as a function of phase shift in Figure 22. It should be observed that this power could probably be reduced by a factor of 3 to 4 by reducing the length of the active (constricted) part of the discharge to less than twice the height of the standard X-band waveguide, which is 1.01 cm. Even then, however, the discharge power required for obtaining a 45 degree phase shift would be several watts.

Slot coupling control by plasma irises. Coupling and loss measurements were conducted on two waveguide-iris configurations which

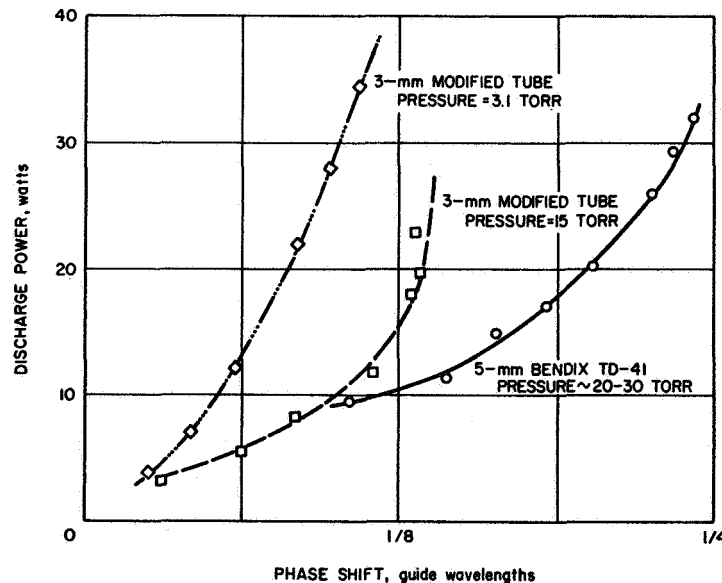


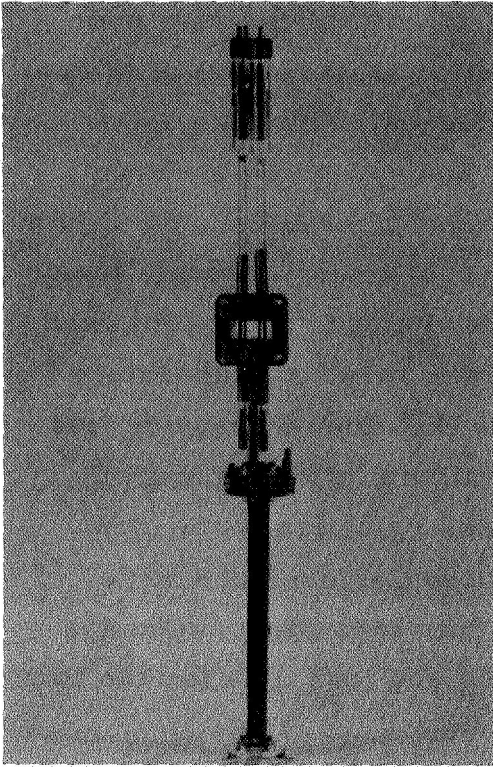
Figure 22. Discharge power versus phase shift for positive column plasma reactance tubes.



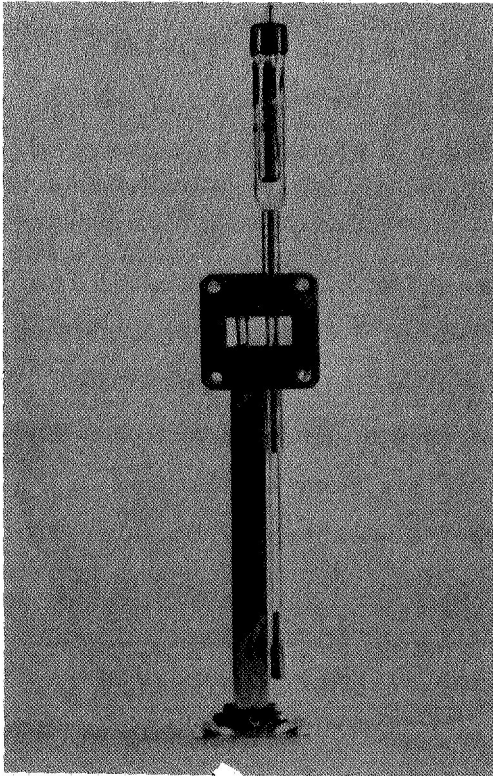
employed positive column plasma varactors to control the amplitude of slot radiation (Figure 23). One configuration (Figure 23a) used two 3-millimeter Bendix tubes (Model TD-42) placed symmetrically and midway along a slot cut on the centerline of the waveguide broadwall. This unit had an inter-tube spacing of 0.5 inch; it produced a maximum slot coupling of -18.3 db, an input VSWR  $< 1.6:1$ , and an ohmic loss variation from 21.2 to 33 percent. The second unit (Figure 23b) used a dummy tube and either a 3-millimeter Bendix tube or a laboratory fabricated, hot cathode 3-millimeter tube as the other waveguide iris. With the Bendix tube the unit provided a maximum slot coupling of -12.4 db, a VSWR  $< 2.0:1$ , and an ohmic loss variation from 13.4 to 21.8 percent. Comparable coupling and loss performance were obtained with the unit using the hot cathode tube containing argon gas at a pressure of 20 Torr. Complete coupling and loss data for the two units are given in Figure 24.

Measured R-F Power Handling Capability. Measurements of the r-f power handling capability were performed with the 5-mm diameter commercial positive column argon discharge tube (Bendix TD-42). The maximum tolerable r-f power was defined as the power for which no change in either the coupled or transmitted r-f signal was observed. This power level was measured to be 10 watts.

Improvement of Positive Column Plasma Varactor. It can be seen from the previous results that an improvement of about 1 order of magnitude in Q is required to make the positive column plasma varactors considered less lossy (higher Q) than a good semiconductor varactor. An improvement in Q would be possible in principle either by the use of a gas with lower electron-neutral collision cross-section or by operation at lower gas pressure. Gases with lower electron-neutral collision cross section, however, also have lower ionization cross sections and therefore require either higher gas pressure or higher discharge current and power to produce a given plasma density. Operation at lower gas pressure for a given gas in the positive column mode requires increased discharge power. This relation was indicated in

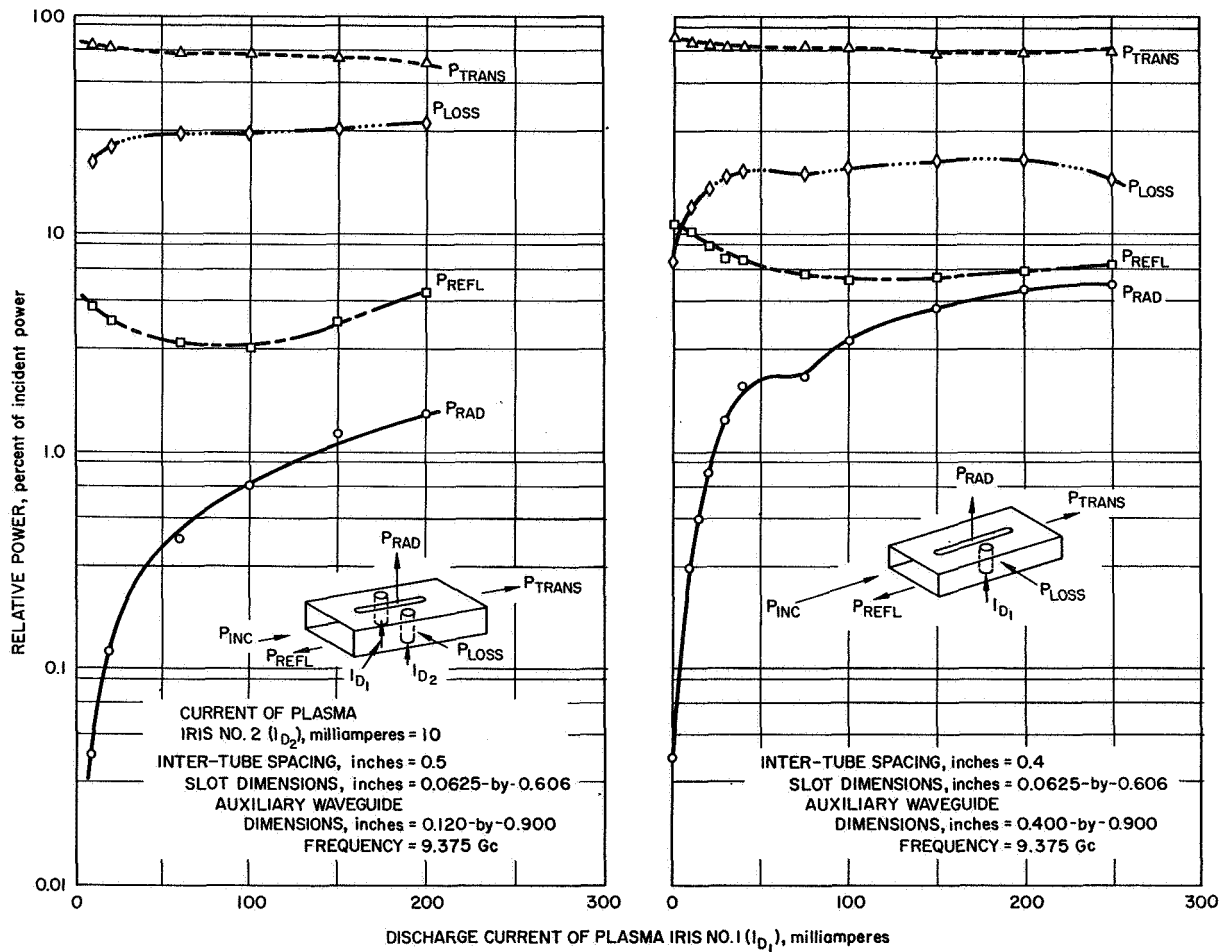


- a. Two Bendix tubes spaced 0.5 inch apart with auxiliary waveguide dimension of 0.120-by-0.900 inch.



- b. One dummy tube and one Bendix tube spaced 0.4 inch apart with auxiliary waveguide dimensions of 0.400-by-0.900 inch.

Figure 23. Variable amplitude control units using 3-millimeter Bendix tubes as irises.



a. For two-Bendix tube unit of Figure 23 a.

b. For dummy tube and one-Bendix tube unit of Figure 23b.

Figure 24. Coupling and loss data for variable amplitude control units using 3-millimeter Bendix tubes as irises.

reference to Figure 20a. In either case, the trade-off for increased Q is an increased discharge power. There is, therefore, little incentive in investigating further the positive column reactance tubes; while somewhat better results than those reported could certainly be obtained by optimizing the gas composition and pressure, the prospective improvements are not important enough to warrant the effort.

#### 2.2.4 Electron Injection Plasma Varactors

The electron injection plasma varactor is characterized by the injection of electrons into the gas to be ionized at an energy level substantially higher than the ionization potential of the gas. Since the electron injection energy is approximately proportional to the applied discharge voltage, it can be externally controlled. An investigation of control techniques for this type of plasma varactor was performed concurrently with the NASA/Langley plasma-iris studies as a Hughes research project.<sup>3,4</sup> Since the results of the investigation complement the NASA studies, they are briefly summarized in this section.

A number of calculations were initially performed on a plasma varactor with a Langmuir mode discharge to obtain data concerning the Q, r-f power handling capability, and discharge power of this type of varactor. Various plasma varactor designs were explored, and the most promising design was incorporated into a single-plasma column coupler. Measurements of the slot coupling obtainable with this kind of control unit were made on several different units using various cathode materials and gases.

A plasma iris with two plasma columns separated by an experimentally determined distance was fabricated to permit both observation of coupling behavior and noise temperature performance and also detection of any interaction between plasma columns. A four-plasma iris test unit was then constructed containing three waveguide ports and pressure-sealed flanges. Variable slot phase and amplitude control were measured with this unit. The studies indicated that an electron injection plasma design can be operated at high r-f power levels with very low ohmic loss. The four-plasma iris prototype developed

displayed 125-watt power handling capability and an average ohmic loss of 5 percent. This unit provided 360 degrees of slot phase control at coupling levels of -13 db and exhibited a VSWR variation below 1.73:1.



### 3.0 CONCLUSIONS

Semiconductor irises which contain horizontally-mounted diodes were shown to exhibit a substantial reduction in ohmic loss, a lower inherent VSWR, and a slight increase in slot phase and amplitude control when compared with previous iris configurations. A 5-slot linear array was built with a 4-diode-iris control device at each slot. Diode-iris phase and amplitude control was demonstrated by scanning the main beam of this array over a 120-degree scan range.

The feasibility of using a plasma iris to control slot radiation was substantiated. Theory and experiments indicated that an electron injection plasma design can be operated at high r-f power levels (>100 watts average) with very low ohmic loss ( $\leq 5$  percent). These findings suggest that further work be performed to develop this design. A comparison of diode and plasma iris characteristics is given in Table III.

	Four-Diode Iris Unit	Four-Plasma Iris Unit (tuner employed in slot arm)
Ohmic loss variation (percent incident power)	14.5 to 8.1	6.5 to 0.0
Amplitude control range (db)	42.2	41.2
Maximum amplitude level (db)	-7.8	-8.8
Phase control range (degrees)	360 (to -14.5 db coupling level)	360 (to -13 db coupling level)
VSWR response	1.13:1 - 1.55:1	1.35:1 to 1.73:1
D-c drive power (watts)	≤0.005	≤63.4
R-f power handling capability (watts)	0.0001	125
Noise temperature (degrees kelvin)	—————	<400

Table III. Comparison of diode and plasma iris characteristics.



#### 4.0 REFERENCES

1. H. E. Shanks and V. Galindo, Ferrite Excited Slots with Controllable Amplitude and Phase. Technical Memorandum 585, Hughes Aircraft Company, January 1960.
2. B. J. Forman, S. N. Vodopia, and W. H. Kummer, Study of Advanced Antenna Techniques for Rendezvous Radar. NASA CR-764, 1967.
3. R. C. Knechtli, J. Y. Wada, and B. J. Forman, Plasma Varactors. Research Report No. 322, Hughes Aircraft Company, Malibu, California, December 1964.
4. B. J. Forman, Plasma Varactors -- Their Use in Several Types of Waveguide Couplers and Phase Shifters. Special Research Study No. SRS-658, Hughes Aircraft Company, Culver City, California, July 1965.
5. D. J. Rose and M. Clark, Plasmas and Controlled Fusion. MIT Press and John Wiley and Sons, New York, 1961.

10-5-67

*"The aeronautical and space activities of the United States shall be conducted so as to contribute . . . to the expansion of human knowledge of phenomena in the atmosphere and space. The Administration shall provide for the widest practicable and appropriate dissemination of information concerning its activities and the results thereof."*

—NATIONAL AERONAUTICS AND SPACE ACT OF 1958

## NASA SCIENTIFIC AND TECHNICAL PUBLICATIONS

**TECHNICAL REPORTS:** Scientific and technical information considered important, complete, and a lasting contribution to existing knowledge.

**TECHNICAL NOTES:** Information less broad in scope but nevertheless of importance as a contribution to existing knowledge.

**TECHNICAL MEMORANDUMS:** Information receiving limited distribution because of preliminary data, security classification, or other reasons.

**CONTRACTOR REPORTS:** Scientific and technical information generated under a NASA contract or grant and considered an important contribution to existing knowledge.

**TECHNICAL TRANSLATIONS:** Information published in a foreign language considered to merit NASA distribution in English.

**SPECIAL PUBLICATIONS:** Information derived from or of value to NASA activities. Publications include conference proceedings, monographs, data compilations, handbooks, sourcebooks, and special bibliographies.

**TECHNOLOGY UTILIZATION PUBLICATIONS:** Information on technology used by NASA that may be of particular interest in commercial and other non-aerospace applications. Publications include Tech Briefs, Technology Utilization Reports and Notes, and Technology Surveys.

*Details on the availability of these publications may be obtained from:*

SCIENTIFIC AND TECHNICAL INFORMATION DIVISION  
NATIONAL AERONAUTICS AND SPACE ADMINISTRATION

Washington, D.C. 20546